Vector radiative transfer equation for arbitrarily shaped and arbitrarily oriented particles: a microphysical derivation from statistical electromagnetics

Michael I. Mishchenko

The concepts of statistical electromagnetics are used to derive the general radiative transfer equation (RTE) that describes multiple scattering of polarized light by sparse discrete random media consisting of arbitrarily shaped and arbitrarily oriented particles. The derivation starts with the volume integral and Lippmann–Schwinger equations for the electric field scattered by a fixed N-particle system and proceeds to the vector form of the Foldy–Lax equations and their approximate far-field version. I then assume that particle positions are completely random and derive the vector RTE by applying the Twersky approximation to the coherent electric field and the Twersky and ladder approximations to the coherency dyad of the diffuse field in the limit $N \to \infty$. The concluding section discusses the physical meaning of the quantities that enter the general vector RTE and the assumptions made in its derivation.

OCIS codes: 030.5620, 260.2110, 260.5430, 280.1310, 290.4210, 290.5850.

1. Introduction

Since the pioneering paper by Schuster,[1] the radiative transfer equation (RTE) has become a classical equation of mathematical physics and has been widely used in diverse areas of science and technology to describe multiple scattering of light by media composed of randomly and sparsely distributed small particles.[2–14] However, introduction of the RTE is usually based on heuristic principles of classical radiometry, i.e., on intuitively appealing considerations of energy balance and the simple phenomenological notions of light rays (i.e., geometric trajectories along which radiant energy is assumed to propagate) and ray pencils. This way to introduce (or, in essence, to postulate) the RTE becomes especially shaky when one tries to include the effects of polarization (the so-called vector RTE, or VRTE) and/or the effects of particle nonsphericity and orientation. Furthermore, it has led to the widespread ignorance of the fact that the real derivation of the RTE and the clarification of the physical meaning of the quantities that enter this equation must be based on fundamental principles of classical electromagnetics as applied to discrete random media.

During the past three decades, there has been significant progress in studies of the statistical wave content of the radiative transfer theory, which has resulted in a much better understanding of the basic assumptions leading to the RTE and has made the latter a corollary of the wave theory (see, e.g., Refs. 15–22 and references therein). However, many of these studies have been limited to multiple scattering of scalar waves and/or to isotropic disordered media, whereas an explicit microphysical derivation of the VRTE from statistical electromagnetics in the case of arbitrarily shaped and arbitrarily oriented particles still appears to be missing. The aim of this paper is to fill this gap.

I begin by briefly summarizing those principles of classical electromagnetics that form the basis of the theory of single light scattering by a small particle. Section 3 forms the main body of the paper and contains a detailed derivation of the general VRTE starting with the vector form of the Foldy–Lax equations for a fixed N-particle system and their far-field version. I then assume that particle positions are completely random and derive the VRTE by applying the Twersky approximation to the coherent electric field and the Twersky and ladder approximations to the coherency dyad of the diffuse (incoherent) field in the limit $N \to \infty$. Section 4 is a summary of the results of the paper and includes a discussion of the physical

The author (crmim@giss.nasa.gov) is with the NASA Goddard Institute for Space Studies, 2880 Broadway, New York, New York 10025.

Received 1 April 2002; revised manuscript received 8 August 2002.

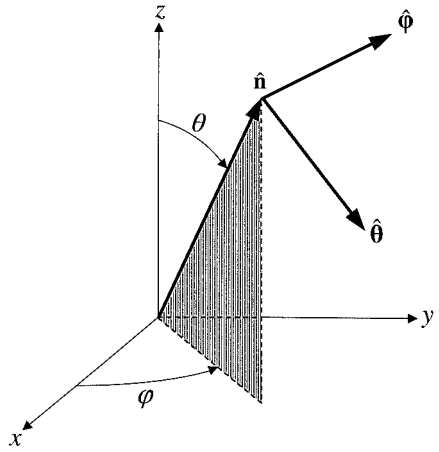

Fig. 1. Local coordinate system used to describe the direction of propagation and the polarization state of a transverse electromagnetic wave at an observation point.

meaning of the quantities that enter the general VRTE and the assumptions made in its derivation. Throughout the paper I assume that the temperature of the particles is low enough that the emitted component of the total radiation field can be neglected.

2. Single Scattering

The aim of this section is to provide a brief introduction of the necessary definitions and notation and to list the equations that will be used in the derivation of the VRTE. An extensive discussion of the subjects covered including explicit derivations of all formulas can be found in Ref. 23. Three-vectors are denoted by use of bold upright letters and matrices are denoted by use of bold sloping letters.

A. Coherency Matrix, Coherency Vector, and Stokes Vector

To introduce various characteristics of a transverse electromagnetic wave, I use the local right-handed Cartesian coordinate system with its origin at the observation point, as shown in Fig. 1, and specify the direction of propagation of the wave by a unit vector $\hat{\mathbf{n}}$ or, alternatively, by a couple $\{\theta, \phi\}$, where $\theta \in [0, \pi]$ is the polar angle measured from the positive z axis and $\phi \in [0, 2\pi)$ is the azimuth angle measured from the positive x axis in the clockwise direction when looking in the direction of the positive z axis. Since the component of the electric field vector along the direction of propagation $\hat{\mathbf{n}}$ is equal to zero, the electric field at the observation point can be expressed as $\mathbf{E} = \mathbf{E}_\theta + \mathbf{E}_\phi$, where $\mathbf{E}_\theta$ and $\mathbf{E}_\phi$ are the θ and ϕ components of the electric field vector, respectively. The component $\mathbf{E}_\theta = E_\theta\hat{\boldsymbol{\theta}}$ lies in the meridional plane (i.e., plane through $\hat{\mathbf{n}}$ and the z axis), whereas the component $\mathbf{E}_\phi = E_\phi\hat{\boldsymbol{\phi}}$ is perpendicular to this plane. $\hat{\boldsymbol{\theta}}$ and $\hat{\boldsymbol{\phi}}$ are the corresponding unit vectors such that $\hat{\mathbf{n}} = \hat{\boldsymbol{\theta}} \times \hat{\boldsymbol{\phi}}$.

Consider a time-harmonic plane electromagnetic wave that propagates in a homogeneous medium with a real electric permittivity ε and a real magnetic susceptibility μ:

$$\mathbf{E}(\mathbf{r}) = \mathbf{E}_0 \exp(ik\hat{\mathbf{n}} \cdot \mathbf{r}), \quad \mathbf{E}_0 \cdot \hat{\mathbf{n}} = 0, \tag{1}$$

where $k = \omega\sqrt{\varepsilon\mu}$ is the (real) wave number and ω is the angular frequency. The 2×2 coherency matrix $\boldsymbol{\rho}$ is defined by

$$\boldsymbol{\rho} = \begin{bmatrix} \rho_{11} & \rho_{12} \\ \rho_{21} & \rho_{22} \end{bmatrix} = \frac{1}{2}\sqrt{\frac{\varepsilon}{\mu}} \begin{bmatrix} E_{0\theta}E_{0\theta}^* & E_{0\theta}E_{0\phi}^* \\ E_{0\phi}E_{0\theta}^* & E_{0\phi}E_{0\phi}^* \end{bmatrix}, \tag{2}$$

where the asterisk denotes a complex conjugate value. The elements of $\boldsymbol{\rho}$ have the dimension of monochromatic energy flux (Wm^{-2}) and can be conveniently grouped into a 4×1 coherency column vector:

$$\boldsymbol{J} = \begin{bmatrix} \rho_{11} \\ \rho_{12} \\ \rho_{21} \\ \rho_{22} \end{bmatrix} = \frac{1}{2}\sqrt{\frac{\varepsilon}{\mu}} \begin{bmatrix} E_{0\theta}E_{0\theta}^* \\ E_{0\theta}E_{0\phi}^* \\ E_{0\phi}E_{0\theta}^* \\ E_{0\phi}E_{0\phi}^* \end{bmatrix}. \tag{3}$$

The Stokes parameters I, Q, U, and V are then defined as the elements of a 4×1 column Stokes vector $\boldsymbol{I}$ as follows:

$$\boldsymbol{I} = \boldsymbol{D}\boldsymbol{J} = \frac{1}{2}\sqrt{\frac{\varepsilon}{\mu}} \begin{bmatrix} E_{0\theta}E_{0\theta}^* + E_{0\phi}E_{0\phi}^* \\ E_{0\theta}E_{0\theta}^* - E_{0\phi}E_{0\phi}^* \\ -E_{0\theta}E_{0\phi}^* - E_{0\phi}E_{0\theta}^* \\ \mathrm{i}(E_{0\phi}E_{0\theta}^* - E_{0\theta}E_{0\phi}^*) \end{bmatrix} = \begin{bmatrix} I \\ Q \\ U \\ V \end{bmatrix}, \tag{4}$$

where

$$\boldsymbol{D} = \begin{bmatrix} 1 & 0 & 0 & 1 \\ 1 & 0 & 0 & -1 \\ 0 & -1 & -1 & 0 \\ 0 & -\mathrm{i} & \mathrm{i} & 0 \end{bmatrix}. \tag{5}$$

B. Volume Integral Equation and Lippmann–Schwinger Equation

Consider a scattering object embedded in an infinite, homogeneous, linear, isotropic, and nonabsorbing medium. The scatterer occupies a finite interior region V_{INT} and is surrounded by the infinite exterior region V_{EXT} such that $V_{\mathrm{INT}} \cup V_{\mathrm{EXT}} = \mathbf{R}^3$. The interior region is filled with an isotropic, linear, and possibly inhomogeneous material.

The monochromatic Maxwell curl equations that describe the scattering of a time-harmonic electromagnetic field are as follows:

$$\left.\begin{aligned} \nabla \times \mathbf{E}(\mathbf{r}) &= \mathrm{i}\omega\mu_1\mathbf{H}(\mathbf{r}) \\ \nabla \times \mathbf{H}(\mathbf{r}) &= -\mathrm{i}\omega\varepsilon_1\mathbf{E}(\mathbf{r}) \end{aligned}\right\} \text{ for } \mathbf{r} \in V_{\mathrm{EXT}}, \tag{6}$$

$$\left.\begin{aligned} \nabla \times \mathbf{E}(\mathbf{r}) &= \mathrm{i}\omega\mu_2(\mathbf{r})\mathbf{H}(\mathbf{r}) \\ \nabla \times \mathbf{H}(\mathbf{r}) &= -\mathrm{i}\omega\varepsilon_2(\mathbf{r})\mathbf{E}(\mathbf{r}) \end{aligned}\right\} \text{ for } \mathbf{r} \in V_{\mathrm{INT}}, \tag{7}$$

where the subscripts 1 and 2 refer to the exterior and interior regions, respectively. Since the first relations in Eqs. (6) and (7) yield the magnetic field provided that the electric field is known everywhere, we

look for the solution of Eqs. (6) and (7) in terms of only the electric field. Assuming that the host medium and the scattering object are nonmagnetic, i.e., $\mu_2(\mathbf{r}) \equiv \mu_1 = \mu_0$, where μ_0 is the permeability of a vacuum, one derives the corresponding vector wave equations:

$$\nabla \times \nabla \times \mathbf{E}(\mathbf{r}) - k_1^2 \mathbf{E}(\mathbf{r}) = 0, \quad \mathbf{r} \in V_{\mathrm{EXT}}, \quad (8)$$

$$\nabla \times \nabla \times \mathbf{E}(\mathbf{r}) - k_2^2(\mathbf{r}) \mathbf{E}(\mathbf{r}) = 0, \quad \mathbf{r} \in V_{\mathrm{INT}}, \quad (9)$$

where $k_1 = \omega\sqrt{\varepsilon_1 \mu_0}$ and $k_2(\mathbf{r}) = \omega\sqrt{\varepsilon_2(\mathbf{r})\mu_0}$ are the wave numbers of the exterior and interior regions, respectively.

Following the approach described in Ref. 23, one can express the solution of Eqs. (8) and (9) in the form of the following volume integral equation:

$$\mathbf{E}(\mathbf{r}) = \mathbf{E}^{\mathrm{inc}}(\mathbf{r}) + k_1^2 \int_{V_{\mathrm{INT}}} \mathrm{d}^3\mathbf{r}' \overleftrightarrow{G}(\mathbf{r}, \mathbf{r}') \cdot \mathbf{E}(\mathbf{r}')[m^2(\mathbf{r}') - 1], \quad \mathbf{r} \in \mathbf{R}^3, \quad (10)$$

where

$$\overleftrightarrow{G}(\mathbf{r}, \mathbf{r}') = \left(\overleftrightarrow{I} + \frac{1}{k_1^2} \nabla \otimes \nabla \right) \frac{\exp(ik_1|\mathbf{r} - \mathbf{r}'|)}{4\pi|\mathbf{r} - \mathbf{r}'|} \quad (11)$$

is the free space dyadic Green's function, $\overleftrightarrow{I}$ is the identity dyad, $\otimes$ denotes the dyadic product of two vectors, and $m(\mathbf{r}) = k_2(\mathbf{r})/k_1$ is the refractive index of the interior relative to that of the exterior. Alternatively, the scattered field $\mathbf{E}^{\mathrm{sca}}(\mathbf{r}) = \mathbf{E}(\mathbf{r}) - \mathbf{E}^{\mathrm{inc}}(\mathbf{r})$ can be expressed in terms of the incident field by means of the dyad transition operator $\overleftrightarrow{T}$:

$$\mathbf{E}^{\mathrm{sca}}(\mathbf{r}) = \int_{V_{\mathrm{INT}}} \mathrm{d}^3\mathbf{r}' \overleftrightarrow{G}(\mathbf{r}, \mathbf{r}') \cdot \int_{V_{\mathrm{INT}}} \mathrm{d}^3\mathbf{r}'' \overleftrightarrow{T}(\mathbf{r}', \mathbf{r}'') \cdot \mathbf{E}^{\mathrm{inc}}(\mathbf{r}''), \quad \mathbf{r} \in \mathbf{R}^3. \quad (12)$$

Substituting Eq. (12) into Eq. (10) yields the Lippmann–Schwinger equation for $\overleftrightarrow{T}$:

$$\overleftrightarrow{T}(\mathbf{r}, \mathbf{r}') = k_1^2[m^2(\mathbf{r}) - 1]\delta(\mathbf{r} - \mathbf{r}')\overleftrightarrow{I} + k_1^2[m^2(\mathbf{r}) - 1] \int_{V_{\mathrm{INT}}} \mathrm{d}^3\mathbf{r}'' \overleftrightarrow{G}(\mathbf{r}, \mathbf{r}'') \cdot \overleftrightarrow{T}(\mathbf{r}'', \mathbf{r}'), \quad \mathbf{r}, \mathbf{r}' \in V_{\mathrm{INT}}. \quad (13)$$

C. Scattering in the Far-Field Zone

Let us choose a point O close to the geometric center of the scattering object as the common origin of all position vectors (Fig. 2) and make the standard far-field-zone assumptions that $k_1 r \gg 1$ and that r is much larger than any linear dimension of the scatterer. Then Eq. (10) becomes

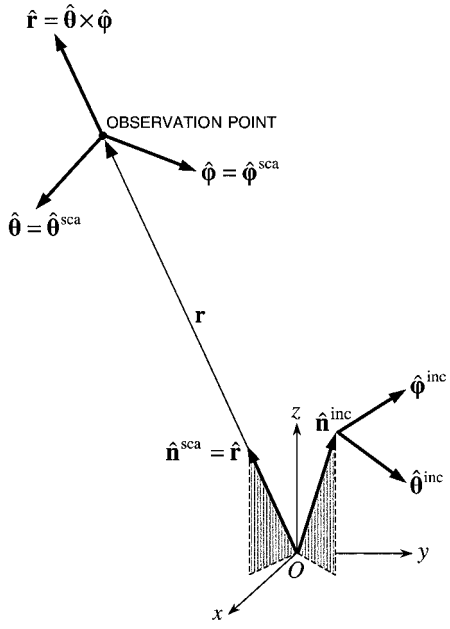

Fig. 2. Scattering in the far-field zone.

$$\mathbf{E}^{\mathrm{sca}}(\mathbf{r}) \underset{r \to \infty}{=} \frac{\exp(ik_1 r)}{r} \frac{k_1^2}{4\pi} (\overleftrightarrow{I} - \hat{\mathbf{r}} \otimes \hat{\mathbf{r}}) \cdot \int_{V_{\mathrm{INT}}} \mathrm{d}^3\mathbf{r}'[m^2(\mathbf{r}') - 1]\mathbf{E}(\mathbf{r}')\exp(-ik_1 \hat{\mathbf{r}} \cdot \mathbf{r}'). \quad (14)$$

The factor $\overleftrightarrow{I} - \hat{\mathbf{r}} \otimes \hat{\mathbf{r}} = \hat{\boldsymbol{\theta}} \otimes \hat{\boldsymbol{\theta}} + \hat{\boldsymbol{\phi}} \otimes \hat{\boldsymbol{\phi}}$ ensures that the scattered spherical wave in the far-field zone is transverse so that

$$\mathbf{E}^{\mathrm{sca}}(\mathbf{r}) \underset{r \to \infty}{=} \frac{\exp(ik_1 r)}{r} \mathbf{E}_1^{\mathrm{sca}}(\hat{\mathbf{r}}), \quad \hat{\mathbf{r}} \cdot \mathbf{E}_1^{\mathrm{sca}}(\hat{\mathbf{r}}) = 0, \quad (15)$$

where the scattering amplitude $\mathbf{E}_1^{\mathrm{sca}}(\hat{\mathbf{r}})$ is independent of r and describes the angular distribution of the scattered radiation.

Assuming that the incident field is a plane electromagnetic wave $\mathbf{E}^{\mathrm{inc}}(\mathbf{r}) = \mathbf{E}_0^{\mathrm{inc}} \exp(ik_1 \hat{\mathbf{n}}^{\mathrm{inc}} \cdot \mathbf{r})$, we have

$$\mathbf{E}_1^{\mathrm{sca}}(\hat{\mathbf{n}}^{\mathrm{sca}}) = \overleftrightarrow{A}(\hat{\mathbf{n}}^{\mathrm{sca}}, \hat{\mathbf{n}}^{\mathrm{inc}}) \cdot \mathbf{E}_0^{\mathrm{inc}}, \quad (16)$$

where $\hat{\mathbf{n}}^{\mathrm{sca}} = \hat{\mathbf{r}}$ (Fig. 2). The elements of the scattering dyad $\overleftrightarrow{A}(\hat{\mathbf{n}}^{\mathrm{sca}}, \hat{\mathbf{n}}^{\mathrm{inc}})$ have the dimension of length. It follows from Eq. (15) that

$$\hat{\mathbf{n}}^{\mathrm{sca}} \cdot \overleftrightarrow{A}(\hat{\mathbf{n}}^{\mathrm{sca}}, \hat{\mathbf{n}}^{\mathrm{inc}}) = 0. \quad (17)$$

Since $\mathbf{E}_0^{\mathrm{inc}} \cdot \hat{\mathbf{n}}^{\mathrm{inc}} = 0$, the dot product $\overleftrightarrow{A}(\hat{\mathbf{n}}^{\mathrm{sca}}, \hat{\mathbf{n}}^{\mathrm{inc}}) \cdot \hat{\mathbf{n}}^{\mathrm{inc}}$ is not defined by Eq. (16). To complete the definition, we take this product to be zero:

$$\overleftrightarrow{A}(\hat{\mathbf{n}}^{\mathrm{sca}}, \hat{\mathbf{n}}^{\mathrm{inc}}) \cdot \hat{\mathbf{n}}^{\mathrm{inc}} = 0. \quad (18)$$

Equations (17) and (18) show that only four out of nine components of the scattering dyad are independent. It is therefore convenient to introduce the 2×2 amplitude matrix $\boldsymbol{S}$, which describes the transformation of the θ and ϕ components of the incident plane wave into the θ and ϕ components of the scattered spherical wave (Fig. 2):

$$\boldsymbol{E}^{\mathrm{sca}}(r\hat{\mathbf{n}}^{\mathrm{sca}}) \underset{r\to\infty}{=} \frac{\exp(\mathrm{i}k_1 r)}{r}\,\boldsymbol{S}(\hat{\mathbf{n}}^{\mathrm{sca}}, \hat{\mathbf{n}}^{\mathrm{inc}})\boldsymbol{E}_0^{\mathrm{inc}}, \quad (19)$$

where $\boldsymbol{E}$ denotes a two-component column formed by the θ and ϕ components of the electric vector. The elements of the amplitude matrix have the dimension of length and are expressed in terms of the scattering dyad as follows:

$$S_{11} = \hat{\boldsymbol{\theta}}^{\mathrm{sca}} \cdot \overleftrightarrow{A} \cdot \hat{\boldsymbol{\theta}}^{\mathrm{inc}}, \quad S_{12} = \hat{\boldsymbol{\theta}}^{\mathrm{sca}} \cdot \overleftrightarrow{A} \cdot \hat{\boldsymbol{\phi}}^{\mathrm{inc}},$$

$$S_{21} = \hat{\boldsymbol{\phi}}^{\mathrm{sca}} \cdot \overleftrightarrow{A} \cdot \hat{\boldsymbol{\theta}}^{\mathrm{inc}}, \quad S_{22} = \hat{\boldsymbol{\phi}}^{\mathrm{sca}} \cdot A \cdot \hat{\boldsymbol{\phi}}^{\mathrm{inc}}. \quad (20)$$

The symmetry of the scattering process with respect to an inversion of time leads to the following reciprocity relations for the scattering dyad and the amplitude matrix:

$$\overleftrightarrow{A}(-\hat{\mathbf{n}}^{\mathrm{inc}}, -\hat{\mathbf{n}}^{\mathrm{sca}}) = \overleftrightarrow{A}^{T}(\hat{\mathbf{n}}^{\mathrm{sca}}, \hat{\mathbf{n}}^{\mathrm{inc}}), \quad (21)$$

$$\boldsymbol{S}(-\hat{\mathbf{n}}^{\mathrm{inc}}, -\hat{\mathbf{n}}^{\mathrm{sca}}) = \begin{bmatrix} S_{11}(\hat{\mathbf{n}}^{\mathrm{sca}}, \hat{\mathbf{n}}^{\mathrm{inc}}) & -S_{21}(\hat{\mathbf{n}}^{\mathrm{sca}}, \hat{\mathbf{n}}^{\mathrm{inc}}) \\ -S_{12}(\hat{\mathbf{n}}^{\mathrm{sca}}, \hat{\mathbf{n}}^{\mathrm{inc}}) & S_{22}(\hat{\mathbf{n}}^{\mathrm{sca}}, \hat{\mathbf{n}}^{\mathrm{inc}}) \end{bmatrix}, \quad (22)$$

where T denotes the transpose of a dyad. Equations (21) and (22) are valid provided that the permeability, permittivity, and conductivity of the scattering object are scalars or symmetric tensors.

D. Phase Matrix

The relationship between the coherency vectors of the incident and the scattered light for scattering directions away from the incidence direction ($\hat{\mathbf{r}} \neq \hat{\mathbf{n}}^{\mathrm{inc}}$) is described by the 4×4 coherency phase matrix $\boldsymbol{Z}^J$:

$$\boldsymbol{J}^{\mathrm{sca}}(r\hat{\mathbf{n}}^{\mathrm{sca}}) = \frac{1}{r^2}\,\boldsymbol{Z}^J(\hat{\mathbf{n}}^{\mathrm{sca}}, \hat{\mathbf{n}}^{\mathrm{inc}})\boldsymbol{J}^{\mathrm{inc}}, \quad (23)$$

where the coherency vectors of the incident plane wave and the scattered spherical wave are defined as

$$\boldsymbol{J}^{\mathrm{inc}} = \frac{1}{2}\sqrt{\frac{\varepsilon_1}{\mu_0}}\begin{pmatrix} E_{0\theta}{}^{\mathrm{inc}}E_{0\theta}{}^{\mathrm{inc}*} \\ E_{0\theta}{}^{\mathrm{inc}}E_{0\phi}{}^{\mathrm{inc}*} \\ E_{0\phi}{}^{\mathrm{inc}}E_{0\theta}{}^{\mathrm{inc}*} \\ E_{0\phi}{}^{\mathrm{inc}}E_{0\phi}{}^{\mathrm{inc}*} \end{pmatrix},$$

$$\boldsymbol{J}^{\mathrm{sca}}(r\hat{\mathbf{n}}^{\mathrm{sca}}) = \frac{1}{r^2}\frac{1}{2}\sqrt{\frac{\varepsilon_1}{\mu_0}}\begin{bmatrix} E_{1\theta}{}^{\mathrm{sca}}(\hat{\mathbf{n}}^{\mathrm{sca}})[E_{1\theta}{}^{\mathrm{sca}}(\hat{\mathbf{n}}^{\mathrm{sca}})]^* \\ E_{1\theta}{}^{\mathrm{sca}}(\hat{\mathbf{n}}^{\mathrm{sca}})[E_{1\phi}{}^{\mathrm{sca}}(\hat{\mathbf{n}}^{\mathrm{sca}})]^* \\ E_{1\phi}{}^{\mathrm{sca}}(\hat{\mathbf{n}}^{\mathrm{sca}})[E_{1\theta}{}^{\mathrm{sca}}(\hat{\mathbf{n}}^{\mathrm{sca}})]^* \\ E_{1\phi}{}^{\mathrm{sca}}(\hat{\mathbf{n}}^{\mathrm{sca}})[E_{1\phi}{}^{\mathrm{sca}}(\hat{\mathbf{n}}^{\mathrm{sca}})]^* \end{bmatrix}, \quad (24)$$

and the elements of $\boldsymbol{Z}^J(\hat{\mathbf{n}}^{\mathrm{sca}}, \hat{\mathbf{n}}^{\mathrm{inc}})$ are quadratic combinations of the elements of the amplitude matrix $\boldsymbol{S}(\hat{\mathbf{n}}^{\mathrm{sca}}, \hat{\mathbf{n}}^{\mathrm{inc}})$:

$$\boldsymbol{Z}^J = \begin{bmatrix} |S_{11}|^2 & S_{11}S_{12}^* & S_{12}S_{11}^* & |S_{12}|^2 \\ S_{11}S_{21}^* & S_{11}S_{22}^* & S_{12}S_{21}^* & S_{12}S_{22}^* \\ S_{21}S_{11}^* & S_{21}S_{12}^* & S_{22}S_{11}^* & S_{22}S_{12}^* \\ |S_{21}|^2 & S_{21}S_{22}^* & S_{22}S_{21}^* & |S_{22}|^2 \end{bmatrix}. \quad (25)$$

The corresponding scattering transformation law in the Stokes vector representation is

$$\boldsymbol{I}^{\mathrm{sca}}(r\hat{\mathbf{n}}^{\mathrm{sca}}) = \frac{1}{r^2}\,\boldsymbol{Z}(\hat{\mathbf{n}}^{\mathrm{sca}}, \hat{\mathbf{n}}^{\mathrm{inc}})\boldsymbol{I}^{\mathrm{inc}}, \quad (26)$$

where $\boldsymbol{I}^{\mathrm{inc}} = \boldsymbol{D}\boldsymbol{J}^{\mathrm{inc}}$ and $\boldsymbol{I}^{\mathrm{sca}} = \boldsymbol{D}\boldsymbol{J}^{\mathrm{sca}}$. The explicit expressions for the elements of the Stokes phase matrix in terms of the amplitude matrix elements follow from Eq. (25) and the obvious formula

$$\boldsymbol{Z}(\hat{\mathbf{n}}^{\mathrm{sca}}, \hat{\mathbf{n}}^{\mathrm{inc}}) = \boldsymbol{D}\boldsymbol{Z}^J(\hat{\mathbf{n}}^{\mathrm{sca}}, \hat{\mathbf{n}}^{\mathrm{inc}})\boldsymbol{D}^{-1}. \quad (27)$$

E. Extinction Matrix

Let us now consider the special case of the exact forward-scattering direction ($\hat{\mathbf{r}} = \hat{\mathbf{n}}^{\mathrm{inc}}$). The coherency vector of the total field for $\hat{\mathbf{r}}$ close to $\hat{\mathbf{n}}^{\mathrm{inc}}$ is defined as

$$\boldsymbol{J}(r\hat{\mathbf{r}}) = \frac{1}{2}\sqrt{\frac{\varepsilon_1}{\mu_0}}\begin{bmatrix} E_\theta(r\hat{\mathbf{r}})[E_\theta(r\hat{\mathbf{r}})]^* \\ E_\theta(r\hat{\mathbf{r}})[E_\phi(r\hat{\mathbf{r}})]^* \\ E_\phi(r\hat{\mathbf{r}})[E_\theta(r\hat{\mathbf{r}})]^* \\ E_\phi(r\hat{\mathbf{r}})[E_\phi(r\hat{\mathbf{r}})]^* \end{bmatrix}, \quad (28)$$

where $\mathbf{E}(r\hat{\mathbf{r}}) = \mathbf{E}^{\mathrm{inc}}(r\hat{\mathbf{r}}) + \mathbf{E}^{\mathrm{sca}}(r\hat{\mathbf{r}})$ is the total electric field. Integrating $\boldsymbol{J}(r\hat{\mathbf{r}})$ over the surface of a collimated detector that faces the incident wave, for the total polarized signal one can obtain

$$\boldsymbol{J}(r\hat{\mathbf{n}}^{\mathrm{inc}})\Delta S = \boldsymbol{J}^{\mathrm{inc}}\Delta S - \boldsymbol{K}^J(\hat{\mathbf{n}}^{\mathrm{inc}})\boldsymbol{J}^{\mathrm{inc}} + \boldsymbol{O}(r^{-2}), \quad (29)$$

where ΔS is the surface area of the detector, and the elements of the 4×4 coherency extinction matrix $\boldsymbol{K}^J(\hat{\mathbf{n}}^{\mathrm{inc}})$ are expressed in terms of the elements of the forward-scattering amplitude matrix $\boldsymbol{S}(\hat{\mathbf{n}}^{\mathrm{inc}}, \hat{\mathbf{n}}^{\mathrm{inc}})$ as follows:

$$\boldsymbol{K}^J = \frac{\mathrm{i}2\pi}{k_1} \times \begin{bmatrix} S_{11}^* - S_{11} & S_{12}^* & -S_{12} & 0 \\ S_{21}^* & S_{22}^* - S_{11} & 0 & -S_{12} \\ -S_{21} & 0 & S_{11}^* - S_{22} & S_{12}^* \\ 0 & -S_{21} & S_{21}^* & S_{22}^* - S_{22} \end{bmatrix}. \quad (30)$$

In the Stokes vector representation,

$$\boldsymbol{I}(r\hat{\mathbf{n}}^{\mathrm{inc}})\Delta S = \boldsymbol{I}^{\mathrm{inc}}\Delta S - \boldsymbol{K}(\hat{\mathbf{n}}^{\mathrm{inc}})\boldsymbol{I}^{\mathrm{inc}} + \boldsymbol{O}(r^{-2}), \quad (31)$$

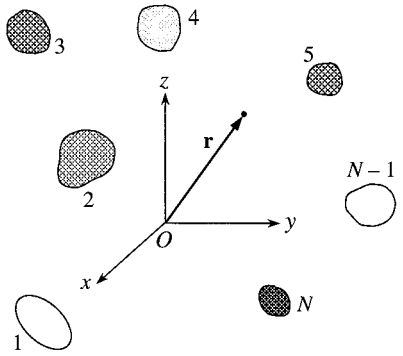

Fig. 3. Scattering by a fixed group of N finite particles.

where $\boldsymbol{I}(r\hat{\mathbf{n}}^{\mathrm{inc}}) = \boldsymbol{DJ}(r\hat{\mathbf{n}}^{\mathrm{inc}})$. Expressions for the elements of the 4×4 Stokes extinction matrix $\boldsymbol{K}(\hat{\mathbf{n}}^{\mathrm{inc}})$ follow from Eq. (30) and the formula

$$\boldsymbol{K}(\hat{\mathbf{n}}^{\mathrm{inc}}) = \boldsymbol{DK}^{J}(\hat{\mathbf{n}}^{\mathrm{inc}})\boldsymbol{D}^{-1}. \tag{32}$$

The reciprocity relation for the Stokes extinction matrix reads

$$\boldsymbol{K}(-\hat{\mathbf{n}}^{\mathrm{inc}}) = \boldsymbol{\Delta}_3[\boldsymbol{K}(\hat{\mathbf{n}}^{\mathrm{inc}})]^{T}\boldsymbol{\Delta}_3, \tag{33}$$

where $\boldsymbol{\Delta}_3 = \mathrm{diag}[1, 1, -1, 1]$ and T denotes the transpose of a matrix.

Equations (29) and (31) represent the most general form of the optical theorem and show that the presence of the scattering particle changes not only the total power of the electromagnetic radiation received by the detector that faces the incident wave, but also, perhaps, its state of polarization. The latter phenomenon is called dichroism and results from different attenuation rates for different polarization components of the incident wave.

3. Multiple Scattering

A. Foldy–Lax Equations

Consider electromagnetic scattering by a fixed group of N finite particles that collectively occupy the interior region $V_{\mathrm{INT}} = \cup_{i=1}^{N} V_i$, where V_i is the (bounded) volume occupied by the ith particle (Fig. 3). The volume integral equation (10) that describes the electric field everywhere in space now reads

$$\mathbf{E}(\mathbf{r}) = \mathbf{E}^{\mathrm{inc}}(\mathbf{r}) + \int_{\mathbf{R}^3} \mathrm{d}^3\mathbf{r}' U(\mathbf{r}') \overleftrightarrow{G}(\mathbf{r}, \mathbf{r}') \cdot \mathbf{E}(\mathbf{r}'), \quad \mathbf{r} \in \mathbf{R}^3, \tag{34}$$

where the integration is performed over the entire space, the potential function $U(\mathbf{r})$ is given by

$$U(\mathbf{r}) = \sum_{i=1}^{N} U_i(\mathbf{r}), \quad \mathbf{r} \in \mathbf{R}^3, \tag{35}$$

and $U_i(\mathbf{r})$ is the ith particle potential function. The latter is given by

$$U_i(\mathbf{r}) = \begin{cases} 0, & \mathbf{r} \notin V_i, \\ k_1^{\,2}[m_i^{\,2}(\mathbf{r}) - 1], & \mathbf{r} \in V_i, \end{cases} \tag{36}$$

where $m_i(\mathbf{r}) = k_{2i}(\mathbf{r})/k_1$ is the refractive index of particle i relative to that of the exterior. All the position vectors originate at origin O of an arbitrarily chosen laboratory coordinate system.

We now show that the total electric field everywhere in space can be expressed as

$$\mathbf{E}(\mathbf{r}) = \mathbf{E}^{\mathrm{inc}}(\mathbf{r}) + \sum_{i=1}^{N} \int_{V_i} \mathrm{d}^3\mathbf{r}' \overleftrightarrow{G}(\mathbf{r}, \mathbf{r}') \cdot \int_{V_i} \mathrm{d}^3\mathbf{r}'' \overleftrightarrow{T}_i(\mathbf{r}', \mathbf{r}'') \cdot \mathbf{E}_i(\mathbf{r}''), \quad \mathbf{r} \in \mathbf{R}^3, \tag{37}$$

where the electric field $\mathbf{E}_i$ exciting particle i is given by

$$\mathbf{E}_i(\mathbf{r}) = \mathbf{E}^{\mathrm{inc}}(\mathbf{r}) + \sum_{j(\neq i)=1}^{N} \mathbf{E}_{ij}^{\mathrm{exc}}(\mathbf{r}), \tag{38a}$$

the $\mathbf{E}_{ij}^{\mathrm{exc}}$ are partial exciting fields given by

$$\mathbf{E}_{ij}^{\mathrm{exc}}(\mathbf{r}) = \int_{V_j} \mathrm{d}^3\mathbf{r}' \overleftrightarrow{G}(\mathbf{r}, \mathbf{r}') \cdot \int_{V_j} \mathrm{d}^3\mathbf{r}'' \overleftrightarrow{T}_j(\mathbf{r}', \mathbf{r}'') \cdot \mathbf{E}_j(\mathbf{r}''), \quad \mathbf{r} \in V_i, \tag{38b}$$

and $\overleftrightarrow{T}_i$ is the ith particle dyad transition operator with respect to the laboratory coordinate system, which satisfies the Lippmann–Schwinger equation

$$\overleftrightarrow{T}_i(\mathbf{r}, \mathbf{r}') = U_i(\mathbf{r})\delta(\mathbf{r} - \mathbf{r}')\overleftrightarrow{I} + U_i(\mathbf{r}) \int_{V_i} \mathrm{d}^3\mathbf{r}'' \overleftrightarrow{G}(\mathbf{r}, \mathbf{r}'') \cdot \overleftrightarrow{T}_i(\mathbf{r}'', \mathbf{r}'), \quad \mathbf{r}, \mathbf{r}' \in V_i. \tag{39}$$

I first introduce the ith potential dyad centered at the origin of the laboratory reference frame,

$$\overleftrightarrow{U}_i(\mathbf{r}, \mathbf{r}') = U_i(\mathbf{r})\delta(\mathbf{r} - \mathbf{r}')\overleftrightarrow{I}, \tag{40}$$

and rewrite Eqs. (34) and (37)–(39) in the following operator form:

$$E = E^{\mathrm{inc}} + \hat{G}\hat{U}E, \tag{41}$$

$$E = E^{\mathrm{inc}} + \sum_{i=1}^{N} \hat{G}\hat{T}_i E_i, \tag{42}$$

$$E_i = E^{\mathrm{inc}} + \sum_{j(\neq i)=1}^{N} \hat{G}\hat{T}_j E_j, \tag{43}$$

$$\hat{T}_i = \hat{U}_i + \hat{U}_i\hat{G}\hat{T}_i, \tag{44}$$

where

$$\hat{U} = \sum_{i=1}^{N} \hat{U}_i, \tag{45}$$

$$\hat{B}E = \int \mathrm{d}^3\mathbf{r}' \overleftrightarrow{B}(\mathbf{r}, \mathbf{r}') \cdot \mathbf{E}(\mathbf{r}'). \tag{46}$$

Equations (45) and (44) yield

$$\hat{U}\hat{G}\hat{T}_i = \hat{U}_i\hat{G}\hat{T}_i + \sum_{j(\neq i)=1}^{N} \hat{U}_j\hat{G}\hat{T}_i = \hat{T}_i - \hat{U}_i + \sum_{j(\neq i)=1}^{N} \hat{U}_j\hat{G}\hat{T}_i. \quad (47)$$

Let us now evaluate the right-hand side of Eq. (41). Substituting sequentially Eqs. (42), (47), and (43) and then again Eq. (42) gives[24]

$$\begin{aligned} E^{\text{inc}} + \hat{G}\hat{U}E &= E^{\text{inc}} + \hat{G}\hat{U}\left(E^{\text{inc}} + \sum_{i=1}^{N} \hat{G}\hat{T}_i E_i\right) \\ &= E^{\text{inc}} + \hat{G}\hat{U}E^{\text{inc}} + \hat{G}\sum_{i=1}^{N} \\ &\quad \times \left(\hat{T}_i - \hat{U}_i + \sum_{j(\neq i)=1}^{N} \hat{U}_j\hat{G}\hat{T}_i\right)E_i \\ &= \left(E^{\text{inc}} + \sum_{i=1}^{N} \hat{G}\hat{T}_i E_i\right) + \hat{G}\hat{U}E^{\text{inc}} \\ &\quad + \hat{G}\sum_{i=1}^{N} \hat{U}_i \sum_{j(\neq i)=1}^{N} \hat{G}\hat{T}_j E_j - \hat{G}\sum_{i=1}^{N} \hat{U}_i E_i \\ &= \left(E^{\text{inc}} + \sum_{i=1}^{N} \hat{G}\hat{T}_i E_i\right) + \hat{G}\hat{U}E^{\text{inc}} \\ &\quad + \hat{G}\sum_{i=1}^{N} \hat{U}_i \left(\sum_{j(\neq i)=1}^{N} \hat{G}\hat{T}_j E_j - E_i\right) \\ &= E^{\text{inc}} + \sum_{i=1}^{N} \hat{G}\hat{T}_i E_i + \hat{G}\hat{U}E^{\text{inc}} \\ &\quad - \hat{G}\sum_{i=1}^{N} \hat{U}_i E^{\text{inc}} = E. \end{aligned} \quad (48)$$

Thus Eqs. (37) and (38) exactly reproduce the volume integral equation (34), which proves their correctness.

Equations (37) and (38) are called the Foldy–Lax equations.[25,26] They directly follow from Maxwell's equations and describe the process of multiple scattering by a fixed group of N particles. Indeed, Eq. (37) expresses the total field everywhere in space in terms of the vector sum of the incident field and the partial fields generated by each particle in response to the corresponding exciting fields, whereas Eqs. (38a) and (38b) show that the field exciting each particle consists of the incident field and the fields generated by all the other particles. Importantly, $\overleftrightarrow{T}_i$ is the dyad transition operator of particle i in the absence of all other particles [see Eqs. (13) and (39)].

B. Far-Field Zone Approximation

I now assume that the distance between any two particles in the group is much larger than the wavelength and much larger than the particle sizes. This means that each particle is located in the far-field zones of all other particles, which allow for considerable simplification of the Foldy–Lax equations. Indeed, according to Eqs. (12), (15), and (38b), the contribution of the jth particle to the field exciting the ith particle in Eq. (38a) can now be represented as a simple outgoing spherical wave centered at the origin of particle j:

$$\mathbf{E}_{ij}^{\text{exc}}(\mathbf{r}) \approx G(r_j)\mathbf{E}_{1ij}(\hat{\mathbf{r}}_j) \approx \exp(-ik_1\hat{\mathbf{R}}_{ij}\cdot\mathbf{R}_i)\mathbf{E}_{ij} \times \exp(ik_1\hat{\mathbf{R}}_{ij}\cdot\mathbf{r}), \quad \mathbf{r}\in V_i, \quad (49)$$

where

$$G(r) = \frac{\exp(ik_1 r)}{r}, \quad (50)$$

$$\mathbf{E}_{ij} = G(R_{ij})\mathbf{E}_{1ij}(\hat{\mathbf{R}}_{ij}), \quad \mathbf{E}_{ij}\cdot\hat{\mathbf{R}}_{ij} = 0,$$

$$\hat{\mathbf{r}}_j = \mathbf{r}_j/r_j, \ \hat{\mathbf{R}}_{ij} = \mathbf{R}_{ij}/R_{ij},$$

$$r_j = |\mathbf{R}_{ij} + \mathbf{r} - \mathbf{R}_i| \underset{R_{ij}\to\infty}{=} R_{ij} + \hat{\mathbf{R}}_{ij}\cdot(\mathbf{r} - \mathbf{R}_i), \quad (51)$$

and the vectors $\mathbf{r}$, $\mathbf{r}_j$, $\mathbf{R}_i$, $\mathbf{R}_j$, and $\mathbf{R}_{ij}$ are shown in Fig. 4(a). Note that we use a lowercase bold letter to denote a vector ending at an observation point, an uppercase bold letter to denote a vector ending at a particle origin, and a caret above a vector to denote a unit vector in the corresponding direction. Obviously, $\mathbf{E}_{ij}$ is the partial exciting field at the origin of the ith particle (i.e., at $\mathbf{r} = \mathbf{R}_i$) caused by the jth particle. Thus, Eq. (38a) and approximation (49) show that each particle is excited by the external field and the superposition of locally plane waves from all other particles with amplitudes $\exp(-ik_1\hat{\mathbf{R}}_{ij}\cdot\mathbf{R}_i)\mathbf{E}_{ij}$ and propagation directions $\hat{\mathbf{R}}_{ij}$:

$$\mathbf{E}_i(\mathbf{r}) \approx \mathbf{E}_0^{\text{inc}}\exp(ik_1\hat{\mathbf{s}}\cdot\mathbf{r}) + \sum_{j(\neq i)=1}^{N} \exp(-ik_1\hat{\mathbf{R}}_{ij}\cdot\mathbf{R}_i)\mathbf{E}_{ij} \times \exp(ik_1\hat{\mathbf{R}}_{ij}\cdot\mathbf{r}), \quad \mathbf{r}\in V_i, \quad (52)$$

where we have assumed that the external incident field is a plane electromagnetic wave:

$$\mathbf{E}^{\text{inc}}(\mathbf{r}) = \mathbf{E}_0^{\text{inc}}\exp(ik_1\hat{\mathbf{s}}\cdot\mathbf{r}), \quad \mathbf{E}_0^{\text{inc}}\cdot\hat{\mathbf{s}} = 0. \quad (53)$$

According to Eqs. (15) and (16), the outgoing spherical wave generated by the jth particle in response to a plane-wave excitation of the form $\mathbf{E}\exp(ik_1\hat{\mathbf{n}}\cdot\mathbf{r}_j)$ is given by $G(r_j)\overleftrightarrow{A}_j(\hat{\mathbf{r}}_j, \hat{\mathbf{n}})\cdot\mathbf{E}$, where $\mathbf{r}_j$ originates at O_j and $\overleftrightarrow{A}_j(\hat{\mathbf{r}}_j, \hat{\mathbf{n}})$ is the jth particle scattering dyad centered at O_j. To exploit this fact, we must rewrite approximation (52) for particle j with respect to the jth particle coordinate system centered at O_j; see Fig. 4(a). Taking into account that $\mathbf{r} = \mathbf{r}_j + \hat{\mathbf{R}}_j$ yields

$$\mathbf{E}_j(\mathbf{r}) \approx \mathbf{E}^{\text{inc}}(\mathbf{R}_j)\exp(ik_1\hat{\mathbf{s}}\cdot\mathbf{r}_j) + \sum_{l(\neq j)=1}^{N} \mathbf{E}_{jl} \times \exp(ik_1\hat{\mathbf{R}}_{jl}\cdot\mathbf{r}_j), \quad \mathbf{r}\in V_j. \quad (54)$$

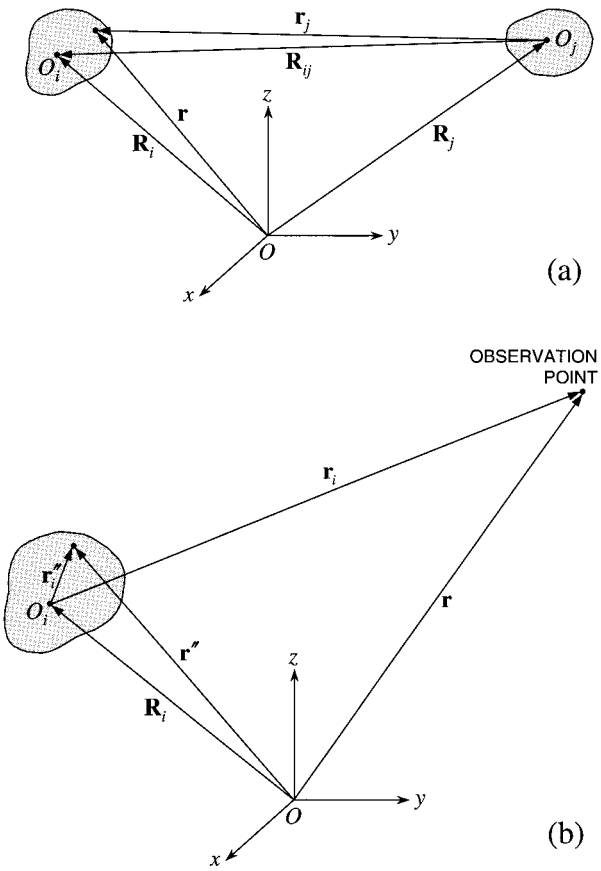

Fig. 4. Scattering by widely separated particles. The local origins O_i and O_j were chosen arbitrarily inside particles i and j, respectively.

The electric field at O_i generated in response to this excitation is simply

$$G(R_{ij}) \times \left[\overleftrightarrow{A}_j(\hat{\mathbf{R}}_{ij}, \hat{\mathbf{s}}) \cdot \mathbf{E}^{\text{inc}}(\mathbf{R}_j) + \sum_{l(\neq j)=1}^{N} \overleftrightarrow{A}_j(\hat{\mathbf{R}}_{ij}, \hat{\mathbf{R}}_{jl}) \cdot \mathbf{E}_{jl} \right]. \tag{55}$$

Equating formula (55) with the right-hand side of approximation (49) evaluated for $\mathbf{r} = \mathbf{R}_i$ finally yields a system of linear algebraic equations for determining the partial exciting fields $\mathbf{E}_{ij}$:

$$\mathbf{E}_{ij} = G(R_{ij}) \left[\overleftrightarrow{A}_j(\hat{\mathbf{R}}_{ij}, \hat{\mathbf{s}}) \cdot \mathbf{E}^{\text{inc}}(\mathbf{R}_j) + \sum_{l(\neq j)=1}^{N} \overleftrightarrow{A}_j(\hat{\mathbf{R}}_{ij}, \hat{\mathbf{R}}_{jl}) \cdot \mathbf{E}_{jl} \right], \quad i, j = 1, \ldots, N, \quad j \neq i. \tag{56}$$

This system is much simpler than the original system of integral equations (38) and can be readily solved on a computer provided that N is not too large.

After the system in Eq. (56) is solved, one can find the electric field exciting each particle and the total field. Indeed, for a point $\mathbf{r}'' \in V_i$ approximation (54) gives

$$\mathbf{E}_i(\mathbf{r}'') \approx \mathbf{E}^{\text{inc}}(\mathbf{R}_i) \exp(\mathrm{i}k_1 \hat{\mathbf{s}} \cdot \mathbf{r}_i'') + \sum_{j(\neq i)=1}^{N} \mathbf{E}_{ij} \times \exp(\mathrm{i}k_1 \hat{\mathbf{R}}_{ij} \cdot \mathbf{r}_i''), \quad \mathbf{r}'' \in V_i \tag{57}$$

[see Fig. 4(b)], which is a vector superposition of plane waves. Substituting $\mathbf{r}_i'' = 0$ in approximation (57) gives a simple formula for the exiting field at the origin of particle i:

$$\mathbf{E}_i(\mathbf{R}_i) = \mathbf{E}^{\text{inc}}(\mathbf{R}_i) + \sum_{j(\neq i)=1}^{N} \mathbf{E}_{ij}. \tag{58}$$

Finally, substituting approximation (57) into Eq. (37) and recalling the mathematical form of the far-field response of a particle to a plane-wave excitation, for the total electric field we derive

$$\mathbf{E}(\mathbf{r}) = \mathbf{E}^{\text{inc}}(\mathbf{r}) + \sum_{i=1}^{N} G(r_i) \overleftrightarrow{A}_i(\hat{\mathbf{r}}_i, \hat{\mathbf{s}}) \cdot \mathbf{E}^{\text{inc}}(\mathbf{R}_i) + \sum_{i=1}^{N} G(r_i) \sum_{j(\neq i)=1}^{N} \overleftrightarrow{A}_i(\hat{\mathbf{r}}_i, \hat{\mathbf{R}}_{ij}) \cdot \mathbf{E}_{ij}, \tag{59}$$

where observation point $\mathbf{r}$, Fig. 4(b), is assumed to be in the far-field zone of any particle that forms the group.

C. Twersky Approximation

Let us now rewrite Eqs. (59) and (56) in a more compact form:

$$\mathbf{E} = \mathbf{E}^{\text{inc}} + \sum_{i=1}^{N} \overleftrightarrow{B}_{ri0} \cdot \mathbf{E}_i^{\text{inc}} + \sum_{i=1}^{N} \sum_{j(\neq i)=1}^{N} \overleftrightarrow{B}_{rij} \cdot \mathbf{E}_{ij}, \tag{60}$$

$$\mathbf{E}_{ij} = \overleftrightarrow{B}_{ij0} \cdot \mathbf{E}_j^{\text{inc}} + \sum_{l(\neq j)=1}^{N} \overleftrightarrow{B}_{ijl} \cdot \mathbf{E}_{jl}, \tag{61}$$

where $\mathbf{E} = \mathbf{E}(\mathbf{r})$, $\mathbf{E}^{\text{inc}} = \mathbf{E}^{\text{inc}}(\mathbf{r})$, $\mathbf{E}_i^{\text{inc}} = \mathbf{E}^{\text{inc}}(\mathbf{R}_i)$,

$$\overleftrightarrow{B}_{ri0} = G(r_i) \overleftrightarrow{A}_i(\hat{\mathbf{r}}_i, \hat{\mathbf{s}}), \quad \overleftrightarrow{B}_{rij} = G(r_i) \overleftrightarrow{A}_i(\hat{\mathbf{r}}_i, \hat{\mathbf{R}}_{ij}),$$
$$\overleftrightarrow{B}_{ij0} = G(R_{ij}) \overleftrightarrow{A}_j(\hat{\mathbf{R}}_{ij}, \hat{\mathbf{s}}), \quad \overleftrightarrow{B}_{ijl} = G(R_{ij}) \overleftrightarrow{A}_j(\hat{\mathbf{R}}_{ij}, \hat{\mathbf{R}}_{jl}). \tag{62}$$

Iterating Eq. (61) yields

$$\mathbf{E}_{ij} = \overleftrightarrow{B}_{ij0} \cdot \mathbf{E}_j^{\text{inc}} + \sum_{\substack{l=1 \\ l \neq j}}^{N} \overleftrightarrow{B}_{ijl} \cdot \overleftrightarrow{B}_{jl0} \cdot \mathbf{E}_l^{\text{inc}} + \sum_{\substack{l=1 \\ l \neq j}}^{N} \sum_{\substack{m=1 \\ m \neq l}}^{N} \overleftrightarrow{B}_{ijl} \cdot \overleftrightarrow{B}_{jlm} \cdot \overleftrightarrow{B}_{lm0} \cdot \mathbf{E}_m^{\text{inc}} + \cdots, \tag{63}$$

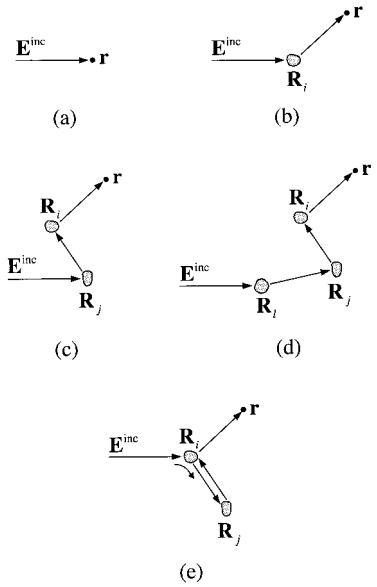

Fig. 5. (a) Incident field, (b) single scattering, (c) double scattering, (d) triple scattering through a self-avoiding path, and (e) triple scattering through a path that goes through particle i twice.

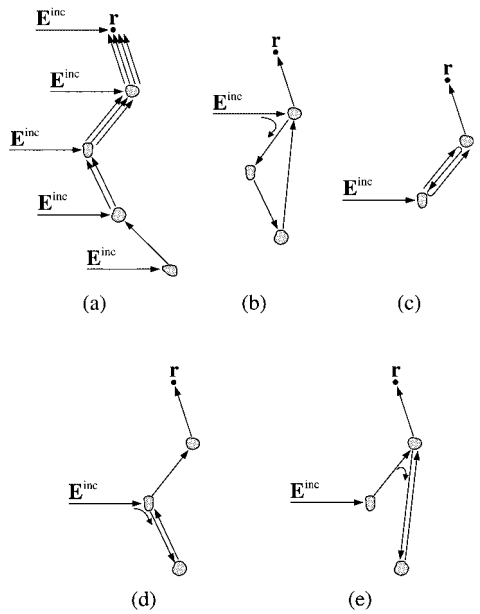

Fig. 6. (a) Self-avoiding scattering paths and (b)–(e) paths that involve four scattering events and go through a particle more than once.

whereas substituting Eq. (63) into Eq. (60) gives an order-of-scattering expansion of the total electric field:

$$\mathbf{E} = \mathbf{E}^{\mathrm{inc}} + \sum_{i=1}^{N} \overleftrightarrow{B}_{ri0} \cdot \mathbf{E}_i^{\mathrm{inc}} + \sum_{i=1}^{N} \sum_{\substack{j=1 \\ j\neq i}}^{N} \overleftrightarrow{B}_{rij} \cdot \overleftrightarrow{B}_{ij0} \cdot \mathbf{E}_j^{\mathrm{inc}} + \sum_{i=1}^{N} \sum_{\substack{j=1 \\ j\neq i}}^{N} \sum_{\substack{l=1 \\ l\neq j}}^{N} \overleftrightarrow{B}_{rij} \cdot \overleftrightarrow{B}_{ijl} \cdot \overleftrightarrow{B}_{jl0} \cdot \mathbf{E}_l^{\mathrm{inc}} + \sum_{i=1}^{N} \sum_{\substack{j=1 \\ j\neq i}}^{N} \sum_{\substack{l=1 \\ l\neq j}}^{N} \sum_{\substack{m=1 \\ m\neq l}}^{N} \overleftrightarrow{B}_{rij} \cdot \overleftrightarrow{B}_{ijl} \cdot \overleftrightarrow{B}_{jlm} \cdot \overleftrightarrow{B}_{lm0} \cdot \mathbf{E}_m^{\mathrm{inc}} + \cdots \tag{64}$$

(see Ref. 27). Indeed, the first term on the right-hand side of Eq. (64) is the incident field, the second term is the sum of all single-scattering contributions, the third term is the sum of all double-scattering contributions, etc., as shown schematically in Fig. 5.

The terms with $j = i$ and $l = j$ in the triple summation on the right-hand side of Eq. (64) are excluded, but the terms with $l = i$ are not. Therefore we can decompose this summation as follows:

$$\sum_{i=1}^{N} \sum_{\substack{j=1 \\ j\neq i}}^{N} \sum_{\substack{l=1 \\ l\neq i \\ l\neq j}}^{N} \overleftrightarrow{B}_{rij} \cdot \overleftrightarrow{B}_{ijl} \cdot \overleftrightarrow{B}_{jl0} \cdot \mathbf{E}_l^{\mathrm{inc}} + \sum_{i=1}^{N} \sum_{\substack{j=1 \\ j\neq i}}^{N} \overleftrightarrow{B}_{rij} \cdot \overleftrightarrow{B}_{iji} \cdot \overleftrightarrow{B}_{ji0} \cdot \mathbf{E}_i^{\mathrm{inc}}. \tag{65}$$

The triple summation in formula (65) is illustrated in Fig. 5(d) and includes scattering paths that go through a particle only once (so-called self-avoiding paths), whereas the double summation involves the paths that go through the same particle more than once, as shown schematically in Fig. 5(e). Higher-order summations in Eq. (64) can be decomposed similarly.

Hence, the total field at an observation point $\mathbf{r}$ is composed of the incident field and single- and multiple-scattering contributions that can be divided into two groups. The first group includes all the terms that correspond to self-avoiding scattering paths, Fig. 6(a), whereas the second group includes all the terms that correspond to the paths that go through a scatterer more than once, Figs. 6(b)–6(e).

The so-called Twersky approximation[27] neglects the terms that belong to the second group and retains only the terms from the first group:

$$\mathbf{E} \approx \mathbf{E}^{\mathrm{inc}} + \sum_{i=1}^{N} \overleftrightarrow{B}_{ri0} \cdot \mathbf{E}_i^{\mathrm{inc}} + \sum_{i=1}^{N} \sum_{\substack{j=1 \\ j\neq i}}^{N} \overleftrightarrow{B}_{rij} \cdot \overleftrightarrow{B}_{ij0} \cdot \mathbf{E}_j^{\mathrm{inc}} + \sum_{i=1}^{N} \sum_{\substack{j=1 \\ j\neq i}}^{N} \sum_{\substack{l=1 \\ l\neq i \\ l\neq j}}^{N} \overleftrightarrow{B}_{rij} \cdot \overleftrightarrow{B}_{ijl} \cdot \overleftrightarrow{B}_{jl0} \cdot \mathbf{E}_l^{\mathrm{inc}} + \sum_{i=1}^{N} \sum_{\substack{j=1 \\ j\neq i}}^{N} \sum_{\substack{l=1 \\ l\neq i \\ l\neq j}}^{N} \sum_{\substack{m=1 \\ m\neq i \\ m\neq j \\ m\neq l}}^{N} \overleftrightarrow{B}_{rij} \cdot \overleftrightarrow{B}_{ijl} \cdot \overleftrightarrow{B}_{jlm} \cdot \overleftrightarrow{B}_{lm0} \cdot \mathbf{E}_m^{\mathrm{inc}} + \cdots. \tag{66}$$

It is straightforward to show that, for a large N, the Twersky approximation includes the majority of multiple-scattering paths. Specifically, a term

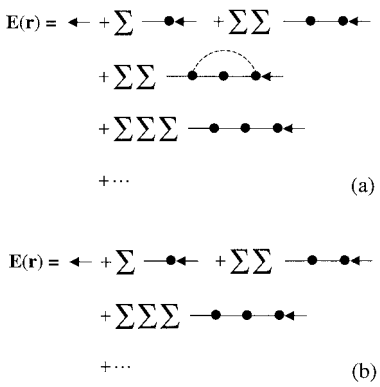

Fig. 7. Diagrammatic representations of (a) Eq. (64) and (b) approximation (66).

with L-nested summations with $L > 2$ on the right-hand side of the exact expansion in Eq. (64) contains $N(N-1)^{L-1}$ terms, whereas that in the approximate expansion contains $N!/(N-L)!$ terms. The ratio of the two numbers indeed tends to unity as $N \to \infty$, which suggests that one can expect the Twersky approximation to yield rather accurate results provided that the number of particles is sufficiently large.

It is convenient to represent order-of-scattering expansions of the electric field by use of the diagram method. Panel (a) of Fig. 7 visualizes the full expansion in Eq. (64), whereas panel (b) illustrates the Twersky approximation (66). The symbol ◀— in these diagrams represents the incident field, the symbol —● denotes multiplying a field by a $\overleftrightarrow{B}$ dyad, and the dashed curve indicates that two scattering events involve the same particle.

D. Statistical Averaging

Although Eqs. (56), (58), and (59) can, in principle, be solved numerically provided that the positions and amplitude matrices of all the particles are known, the solution becomes increasingly time-consuming and eventually impracticable with growing N. Furthermore, one is often interested in electromagnetic scattering by a large group of randomly positioned particles. Although the latter can be studied by computing the scattered field for many different fixed spatial configurations of particles and then taking the ensemble average, a more efficient approach is for one to use methods of statistical electromagnetics. Specifically, it is convenient to describe a large group of N arbitrarily oriented particles randomly distributed throughout a volume V by use of the probability density function $p(\mathbf{R}_1, \xi_1; \ldots; \mathbf{R}_i, \xi_i; \ldots; \mathbf{R}_N, \xi_N)$. The probability of finding the first particle in the volume element $\mathrm{d}^3\mathbf{R}_1$ centered at $\mathbf{R}_1$ and with its state in the region $\mathrm{d}\xi_1$ centered at $\xi_1, \ldots$, the ith particle in the volume element $\mathrm{d}^3\mathbf{R}_i$ centered at $\mathbf{R}_i$ and with its state in the region $\mathrm{d}\xi_i$ centered at $\xi_i, \ldots$, and the Nth particle in the volume element $\mathrm{d}^3\mathbf{R}_N$ centered at $\mathbf{R}_N$ and with its state in the region $\mathrm{d}\xi_N$ centered at ξ_N is given by

$$p(\mathbf{R}_1, \xi_1; \ldots; \mathbf{R}_i, \xi_i; \ldots; \mathbf{R}_N, \xi_N) \prod_{i=1}^{N} \mathrm{d}^3\mathbf{R}_i \mathrm{d}\xi_i. \quad (67)$$

The state of a particle can collectively indicate its size, refractive index, shape, orientation, etc. The probability density function is normalized to unity:

$$\int p(\mathbf{R}_1, \xi_1; \ldots; \mathbf{R}_i, \xi_i; \ldots; \mathbf{R}_N, \xi_N) \prod_{i=1}^{N} \mathrm{d}^3\mathbf{R}_i \mathrm{d}\xi_i = 1, \quad (68)$$

where the integration is performed over the entire range of particle positions and states. The statistical average of a random function f depending on all N particles is given by

$$\langle f \rangle = \int f(\mathbf{R}_1, \xi_1; \ldots; \mathbf{R}_i, \xi_i; \ldots; \mathbf{R}_N, \xi_N) \times p(\mathbf{R}_1, \xi_1; \ldots; \mathbf{R}_i, \xi_i; \ldots; \mathbf{R}_N, \xi_N) \prod_{i=1}^{N} \mathrm{d}^3\mathbf{R}_i \mathrm{d}\xi_i. \quad (69)$$

If the position and state of each particle are independent of those of all other particles then

$$p(\mathbf{R}_1, \xi_1; \ldots; \mathbf{R}_i, \xi_i; \ldots; \mathbf{R}_N, \xi_N) = \prod_{i=1}^{N} p_i(\mathbf{R}_i, \xi_i). \quad (70)$$

This is a good approximation when particles are sparsely distributed so that the finite size of the particles can be neglected. In this case the effect of size appears only in the particle scattering characteristics. If, furthermore, the state of each particle is independent of its position, then

$$p_i(\mathbf{R}_i, \xi_i) = p_{\mathbf{R}i}(\mathbf{R}_i) p_{\xi i}(\xi_i). \quad (71)$$

Finally, assuming that all particles have the same statistical characteristics, we have

$$p_i(\mathbf{R}_i, \xi_i) \equiv p(\mathbf{R}_i, \xi_i) = p_{\mathbf{R}}(\mathbf{R}_i) p_{\xi}(\xi_i), \quad (72)$$

$$\int p_{\mathbf{R}}(\mathbf{R}) \mathrm{d}^3\mathbf{R} = 1, \qquad \int p_{\xi}(\xi) \mathrm{d}\xi = 1. \quad (73)$$

The interpretation of the probability density function $p_{\mathbf{R}}(\mathbf{R})$ is simple:

$$\begin{aligned} p_{\mathbf{R}}(\mathbf{R}) \mathrm{d}^3\mathbf{R} &= \text{probability of finding a particle within volume } \mathrm{d}^3\mathbf{R} \text{ centered at } \mathbf{R} \\ &= \frac{\text{number of particles within } \mathrm{d}^3\mathbf{R}}{\text{total number of particles}} \\ &= \frac{n_0(\mathbf{R}) \mathrm{d}^3\mathbf{R}}{N}, \end{aligned} \quad (74)$$

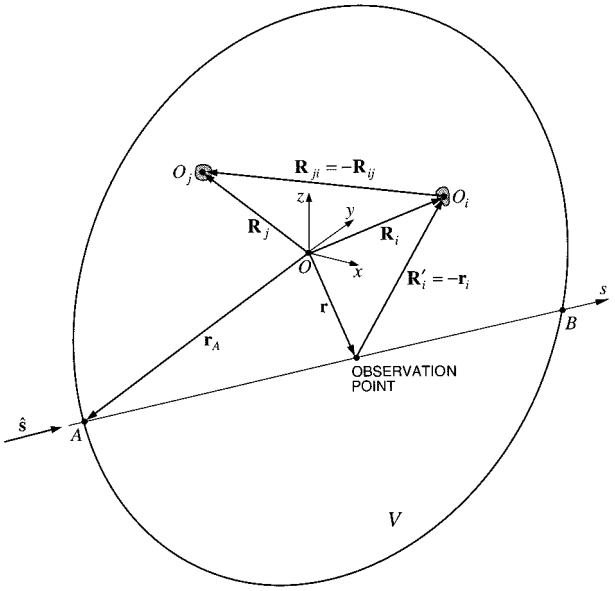

Fig. 8. Geometry showing the quantities used in the derivation of Eq. (86).

where $n_0(\mathbf{R})$ is the local particle number density defined as the number of particles per unit volume in the vicinity of $\mathbf{R}$. Thus

$$p_{\mathbf{R}}(\mathbf{R}) = n_0(\mathbf{R})/N. \tag{75}$$

If the spatial distribution of the N particles throughout volume V is statistically uniform then

$$n_0(\mathbf{R}) \equiv n_0 = N/V, \qquad p_{\mathbf{R}}(\mathbf{R}) = 1/V. \tag{76}$$

E. Coherent Field

Let us consider the electric field $\mathbf{E}(\mathbf{r})$ at a point $\mathbf{r}$ in a medium composed of a large number N of randomly distributed particles. In general, $\mathbf{E}(\mathbf{r})$ is a random function of $\mathbf{r}$ and of the time-dependent coordinates and states of the particles and can be decomposed into the average (or coherent) field $\mathbf{E}_c(\mathbf{r})$ and the fluctuating field $\mathbf{E}_f(\mathbf{r})$:

$$\mathbf{E}(\mathbf{r}) = \mathbf{E}_c(\mathbf{r}) + \mathbf{E}_f(\mathbf{r}), \quad \mathbf{E}_c(\mathbf{r}) = \langle \mathbf{E}(\mathbf{r}) \rangle, \quad \langle \mathbf{E}_f(\mathbf{r}) \rangle = 0. \tag{77}$$

The statistical averaging is performed over physically realizable coordinates and states of all the particles. Assuming that the particles are sparsely distributed and have the same statistical characteristics, from approximation (66) and Eqs. (62), (70), and (72) we have

$$\begin{aligned}\mathbf{E}_c = \mathbf{E}^{\text{inc}} &+ \sum_{i=1}^{N} \int \langle \overleftrightarrow{A}(\hat{\mathbf{r}}_i, \hat{\mathbf{s}}) \rangle \cdot \mathbf{E}_i^{\text{inc}} G(r_i) p_{\mathbf{R}}(\mathbf{R}_i) \mathrm{d}^3\mathbf{R}_i \\ &+ \sum_{i=1}^{N} \sum_{\substack{j=1 \\ j \neq i}}^{N} \int \langle \overleftrightarrow{A}(\hat{\mathbf{r}}_i, \hat{\mathbf{R}}_{ij}) \rangle \cdot \langle \overleftrightarrow{A}(\hat{\mathbf{R}}_{ij}, \hat{\mathbf{s}}) \rangle \\ &\cdot \mathbf{E}_j^{\text{inc}} G(r_i) G(R_{ij}) p_{\mathbf{R}}(\mathbf{R}_i) p_{\mathbf{R}}(\mathbf{R}_j) \mathrm{d}^3\mathbf{R}_i \mathrm{d}^3\mathbf{R}_j + \cdots,\end{aligned} \tag{78}$$

where $\langle \overleftrightarrow{A}(\hat{\mathbf{m}}, \hat{\mathbf{n}}) \rangle$ is the average of the scattering dyad over the particle states. Finally, recalling Eq. (75), in the limit $N \to \infty$ we obtain

$$\begin{aligned}\mathbf{E}_c = \mathbf{E}^{\text{inc}} &+ \frac{N}{N} \int \langle \overleftrightarrow{A}(\hat{\mathbf{r}}_i, \hat{\mathbf{s}}) \rangle \cdot \mathbf{E}_i^{\text{inc}} G(r_i) n_0(\mathbf{R}_i) \mathrm{d}^3\mathbf{R}_i \\ &+ \frac{N(N-1)}{N^2} \int \langle \overleftrightarrow{A}(\hat{\mathbf{r}}_i, \hat{\mathbf{R}}_{ij}) \rangle \cdot \langle \overleftrightarrow{A}(\hat{\mathbf{R}}_{ij}, \hat{\mathbf{s}}) \rangle \\ &\cdot \mathbf{E}_j^{\text{inc}} G(r_i) G(R_{ij}) n_0(\mathbf{R}_i) n_0(\mathbf{R}_j) \mathrm{d}^3\mathbf{R}_i \mathrm{d}^3\mathbf{R}_j \\ &+ \cdots\end{aligned} \tag{79a}$$

$$\begin{aligned}&\underset{N \to \infty}{=} \mathbf{E}^{\text{inc}} + \int \langle \overleftrightarrow{A}(\hat{\mathbf{r}}_i, \hat{\mathbf{s}}) \rangle \cdot \mathbf{E}_i^{\text{inc}} G(r_i) n_0(\mathbf{R}_i) \mathrm{d}^3\mathbf{R}_i \\ &+ \int \langle A(\hat{\mathbf{r}}_i, \hat{\mathbf{R}}_{ij}) \rangle \cdot \langle \overleftrightarrow{A}(\hat{\mathbf{R}}_{ij}, \hat{\mathbf{s}}) \rangle \\ &\cdot \mathbf{E}_j^{\text{inc}} G(r_i) G(R_{ij}) n_0(\mathbf{R}_i) n_0(\mathbf{R}_j) \mathrm{d}^3\mathbf{R}_i \mathrm{d}^3\mathbf{R}_j + \cdots,\end{aligned} \tag{79b}$$

where we have replaced all factors $(N-n)!/N!$ by N^n. This is the general vector form of the expansion derived by Twersky[27] for scalar waves.

I now use Eqs. (79) to compute the coherent field at an observation point inside a discrete random medium that occupies a large volume V and is illuminated by a plane electromagnetic wave incident in direction $\hat{\mathbf{s}}$. For simplicity, we assume that the particles are distributed uniformly throughout the volume so that $n_0(\mathbf{R}) \equiv n_0$ and that the medium has a concave boundary. The latter assumption ensures that all the points of a straight line that connects any two points of the medium lie inside the medium. It is convenient for our purposes to introduce an s axis parallel to the incidence direction and going through the observation point. This axis enters volume V at point A such that $s(A) = 0$ and exits it at point B (Fig. 8). Let us denote the first integral in Eq. (79b) as $\mathbf{I}_1$. From $\mathbf{R}_i = \mathbf{r} + \mathbf{R}_i'$, we have

$$\begin{aligned}\mathbf{I}_1 = n_0 &\int_V \mathrm{d}^3\mathbf{R}_i' \exp(\mathrm{i}k_1 \hat{\mathbf{s}} \cdot \mathbf{R}_i') \\ &\times \frac{\exp(\mathrm{i}k_1 R_i')}{R_i'} \langle \overleftrightarrow{A}(-\hat{\mathbf{R}}_i', \hat{\mathbf{s}}) \rangle \cdot \mathbf{E}^{\text{inc}}(\mathbf{r}).\end{aligned} \tag{80}$$

The observation point is assumed to be in the far-field zone of any particle, which means that $k_1 R_i' \gg 1$. In Eq. (80) we can, therefore, use the asymptotic expansion of a plane wave in spherical waves[28]:

$$\begin{aligned}\exp(\mathrm{i}k_1 \hat{\mathbf{s}} \cdot \mathbf{R}_i') &\underset{k_1 R_i' \to \infty}{=} \frac{i2\pi}{k_1 R_i'} [\delta(\hat{\mathbf{s}} + \hat{\mathbf{R}}_i') \exp(-\mathrm{i}k_1 R_i') \\ &- \delta(\hat{\mathbf{s}} - \hat{\mathbf{R}}_i') \exp(\mathrm{i}k_1 R_i')].\end{aligned} \tag{81}$$

To evaluate the integral in Eq. (80), we use a spherical coordinate system with origin at the observation

point and with the z axis directed along the s axis. We thus have

$$\mathbf{I}_1 = \frac{\mathrm{i}2\pi n_0}{k_1}\int_{4\pi} \mathrm{d}\hat{\mathbf{R}}_i' \int \mathrm{d}R_i' \langle \overleftrightarrow{A}(-\hat{\mathbf{R}}_i', \hat{\mathbf{s}})\rangle \cdot \mathbf{E}^{\mathrm{inc}}(\mathbf{r})[\delta(\hat{\mathbf{s}} + \hat{\mathbf{R}}_i') - \delta(\hat{\mathbf{s}} - \hat{\mathbf{R}}_i')\exp(2\mathrm{i}k_1 R_i')] \approx \frac{\mathrm{i}2\pi n_0}{k_1} s(\mathbf{r})\langle \overleftrightarrow{A}(\hat{\mathbf{s}}, \hat{\mathbf{s}})\rangle \cdot \mathbf{E}^{\mathrm{inc}}(\mathbf{r}), \quad (82)$$

where we have taken into account that $s(\mathbf{r}) \gg 1/k_1$.

Consider now the second integral in Eq. (79b) and denote it $\mathbf{I}_2$. Since $\mathbf{R}_j = \mathbf{r} + \mathbf{R}_i' + \mathbf{R}_{ji}$, we have

$$\mathbf{I}_2 = {n_0}^2 \int \mathrm{d}R_i' R_i'^2 G(R_i') \int_{4\pi} \mathrm{d}\hat{\mathbf{R}}_i' \int \mathrm{d}R_{ji} R_{ji}^2 G(R_{ji}) \times \int_{4\pi} \mathrm{d}\hat{\mathbf{R}}_{ji} \langle \overleftrightarrow{A}(-\hat{\mathbf{R}}_i', -\hat{\mathbf{R}}_{ji})\rangle \cdot \langle \overleftrightarrow{A}(-\hat{\mathbf{R}}_{ji}, \hat{\mathbf{s}})\rangle \cdot \mathbf{E}_j^{\mathrm{inc}}, \quad (83)$$

where

$$\begin{aligned}\mathbf{E}_j^{\mathrm{inc}} &= \exp(\mathrm{i}k_1\hat{\mathbf{s}} \cdot \mathbf{R}_j)\mathbf{E}_0^{\mathrm{inc}} = \exp(\mathrm{i}k_1\hat{\mathbf{s}} \cdot \mathbf{R}_i') \times \exp(\mathrm{i}k_1\hat{\mathbf{s}} \cdot \mathbf{R}_{ji})\mathbf{E}^{\mathrm{inc}}(\mathbf{r}) \\ &= \left(\frac{\mathrm{i}2\pi}{k_1}\right)^2 \frac{1}{R_i'}[\delta(\hat{\mathbf{s}} + \hat{\mathbf{R}}_i')\exp(-\mathrm{i}k_1 R_i') - \delta(\hat{\mathbf{s}} - \hat{\mathbf{R}}_i')\exp(\mathrm{i}k_1 R_i')] \\ &\quad \times \frac{1}{R_{ji}}[\delta(\hat{\mathbf{s}} + \hat{\mathbf{R}}_{ji})\exp(-\mathrm{i}k_1 R_{ji}) - \delta(\hat{\mathbf{s}} - \hat{\mathbf{R}}_{ji})\exp(\mathrm{i}k_1 R_{ji})]\mathbf{E}^{\mathrm{inc}}(\mathbf{r}). \quad (84)\end{aligned}$$

It is thus clear that only particles with origins on the s axis contribute to $\mathbf{I}_2$. Substituting Eq. (84) into Eq. (83) yields

$$\mathbf{I}_2 = \frac{1}{2}\left[\frac{\mathrm{i}2\pi n_0}{k_1} s(\mathbf{r})\right]^2 \langle \overleftrightarrow{A}(\hat{\mathbf{s}}, \hat{\mathbf{s}})\rangle \cdot \langle \overleftrightarrow{A}(\hat{\mathbf{s}}, \hat{\mathbf{s}})\rangle \cdot \mathbf{E}^{\mathrm{inc}}(\mathbf{r}). \quad (85)$$

The remaining integrals in Eq. (79b) are evaluated analogously. The final result is

$$\mathbf{E}_c(\mathbf{r}) = \exp\left[\frac{\mathrm{i}2\pi n_0}{k_1} s(\mathbf{r})\langle \overleftrightarrow{A}(\hat{\mathbf{s}}, \hat{\mathbf{s}})\rangle\right] \cdot \mathbf{E}^{\mathrm{inc}}(\mathbf{r}), \quad (86)$$

where the dyadic exponent is defined as $\exp(\overleftrightarrow{B}) = \overleftrightarrow{I} + \overleftrightarrow{B} + (1/2!)\overleftrightarrow{B} \cdot \overleftrightarrow{B} + (1/3!)\overleftrightarrow{B} \cdot \overleftrightarrow{B} \cdot \overleftrightarrow{B} + \cdots$. Since $\mathbf{r} = \mathbf{r}_A + s(\mathbf{r})\hat{\mathbf{s}}$ (Fig. 8), we have

$$\begin{aligned}\mathbf{E}_c(\mathbf{r}) &= \exp[\mathrm{i}\overleftrightarrow{\kappa}(\hat{\mathbf{s}})s(\mathbf{r})] \cdot \mathbf{E}^{\mathrm{inc}}(\mathbf{r}_A) \\ &= \overleftrightarrow{\eta}[\hat{\mathbf{s}}, s(\mathbf{r})] \cdot \mathbf{E}^{\mathrm{inc}}(\mathbf{r}_A), \quad (87)\end{aligned}$$

where

$$\overleftrightarrow{\kappa}(\hat{\mathbf{s}}) = k_1\overleftrightarrow{I} + \frac{2\pi n_0}{k_1}\langle \overleftrightarrow{A}(\hat{\mathbf{s}}, \hat{\mathbf{s}})\rangle \quad (88)$$

is the dyadic propagation constant for the propagation direction $\hat{\mathbf{s}}$ and

$$\overleftrightarrow{\eta}(\hat{\mathbf{s}}, s) = \exp[\mathrm{i}\overleftrightarrow{\kappa}(\hat{\mathbf{s}})s] \quad (89)$$

is the coherent transmission dyad. This is the general vector form of the Foldy approximation for the coherent field.[25] Tsang and Kong[21] derived it using a different approach. Another form of Eq. (87) is

$$\frac{\mathrm{d}\mathbf{E}_c(\mathbf{r})}{\mathrm{d}s} = \mathrm{i}\overleftrightarrow{\kappa}(\hat{\mathbf{s}}) \cdot \mathbf{E}_c(\mathbf{r}). \quad (90)$$

The coherent field also satisfies the vector Helmholtz equation

$$\nabla^2\mathbf{E}_c(\mathbf{r}) + {k_1}^2\overleftrightarrow{\varepsilon}(\hat{\mathbf{s}}) \cdot \mathbf{E}_c(\mathbf{r}) = 0, \quad (91)$$

where $\overleftrightarrow{\varepsilon}(\hat{\mathbf{s}}) = \overleftrightarrow{I} + 4\pi n_0 {k_1}^{-2}\langle \overleftrightarrow{A}(\hat{\mathbf{s}}, \hat{\mathbf{s}})\rangle$ is the effective dyadic dielectric constant.

These results have several important implications. First, they show that the coherent field is a wave that propagates in the direction of incident field $\hat{\mathbf{s}}$. Second, since the products $\langle \overleftrightarrow{A}(\hat{\mathbf{s}}, \hat{\mathbf{s}})\rangle \cdot \mathbf{E}_0^{\mathrm{inc}}$, $\langle \overleftrightarrow{A}(\hat{\mathbf{s}}, \hat{\mathbf{s}})\rangle \cdot \langle \overleftrightarrow{A}(\hat{\mathbf{s}}, \hat{\mathbf{s}})\rangle \cdot \mathbf{E}_0^{\mathrm{inc}}$, etc. always give electric vectors perpendicular to $\hat{\mathbf{s}}$, the coherent wave is transverse: $\mathbf{E}_c(\mathbf{r}) \cdot \hat{\mathbf{s}} = 0$. Third, Eq. (88) generalizes the optical theorem to the case of many scatterers by expressing the dyadic propagation constant in terms of the forward-scattering amplitude matrix averaged over the particle ensemble.

We can exploit the transverse character of the coherent wave to rewrite the above equations in a simpler matrix form. As in Section 2, we characterize the direction of propagation $\hat{\mathbf{s}}$ at observation point $\mathbf{r}$ using the corresponding polar and azimuth angles in the local coordinate system centered at the observation point and having the same spatial orientation as the laboratory coordinate system $\{x, y, z\}$ (Fig. 8). Then the electric vector of the transverse coherent wave can be written as the vector sum of the corresponding θ and ϕ components: $\mathbf{E}_c(\mathbf{r}) = E_{c\theta}(\mathbf{r})\hat{\boldsymbol{\theta}} + E_{c\phi}(\mathbf{r})\hat{\boldsymbol{\phi}}$. Denoting the two-component electric column vector of the coherent field as $\boldsymbol{E}_c(\mathbf{r})$, instead of Eq. (90) we have

$$\frac{\mathrm{d}\boldsymbol{E}_c(\mathbf{r})}{\mathrm{d}s} = \mathrm{i}\boldsymbol{k}(\hat{\mathbf{s}})\boldsymbol{E}_c(\mathbf{r}), \quad (92)$$

where $\boldsymbol{k}(\hat{\mathbf{s}})$ is the 2×2 matrix propagation constant with elements

$$\begin{aligned}k_{11}(\hat{\mathbf{s}}) &= \hat{\boldsymbol{\theta}}(\hat{\mathbf{s}}) \cdot \overleftrightarrow{\kappa}(\hat{\mathbf{s}}) \cdot \hat{\boldsymbol{\theta}}(\hat{\mathbf{s}}), \\ k_{12}(\hat{\mathbf{s}}) &= \hat{\boldsymbol{\theta}}(\hat{\mathbf{s}}) \cdot \overleftrightarrow{\kappa}(\hat{\mathbf{s}}) \cdot \hat{\boldsymbol{\phi}}(\hat{\mathbf{s}}), \\ k_{21}(\hat{\mathbf{s}}) &= \hat{\boldsymbol{\phi}}(\hat{\mathbf{s}}) \cdot \overleftrightarrow{\kappa}(\hat{\mathbf{s}}) \cdot \hat{\boldsymbol{\theta}}(\hat{\mathbf{s}}), \\ k_{22}(\hat{\mathbf{s}}) &= \hat{\boldsymbol{\phi}}(\hat{\mathbf{s}}) \cdot \overleftrightarrow{\kappa}(\hat{\mathbf{s}}) \cdot \hat{\boldsymbol{\phi}}(\hat{\mathbf{s}}). \quad (93)\end{aligned}$$

Obviously,

$$\boldsymbol{k}(\hat{\mathbf{s}}) = k_1 \mathrm{diag}[1,\ 1] + \frac{2\pi n_0}{k_1}\langle \boldsymbol{S}(\hat{\mathbf{s}},\ \hat{\mathbf{s}})\rangle, \qquad (94)$$

where $\langle \boldsymbol{S}(\hat{\mathbf{s}},\ \hat{\mathbf{s}})\rangle$ is the forward-scattering amplitude matrix averaged over the particle states.

The fact that the propagation of the coherent field is controlled by the forward-scattering amplitude matrix is not surprising. Indeed, the fluctuating component of the total field is the vector sum of the partial fields generated by different particles. Random movements of the particles involve large phase shifts in the partial fields, thereby causing the fluctuating field to disappear when it is averaged over particle positions. The exact forward-scattering direction is different because, in any plane parallel to the incident wave front, the phase of the partial wave forward scattered by a particle in response to the incident wave does not depend on the particle position. Therefore, the interference of the incident wave and the forward-scattered partial wave is always the same regardless of the precise position of the particle inside the medium, and the result of the interference does not vanish after statistical averaging over all particle positions.

It is often convenient to rewrite Eq. (92) in the form

$$\boldsymbol{E}_c(s) = \boldsymbol{h}(\hat{\mathbf{s}},\ s)\ \cdot\ \boldsymbol{E}_c(0), \qquad (95)$$

where

$$\boldsymbol{h}(\hat{\mathbf{s}},\ s) = \exp[\mathrm{i}\boldsymbol{k}(\hat{\mathbf{s}})s] \qquad (96)$$

is the coherent transmission amplitude matrix. From the reciprocity relations (21) and (22), we easily derive the following reciprocity relations for the coherent transmission dyad and the coherent transmission amplitude matrix:

$$\overleftrightarrow{\eta}(-\hat{\mathbf{s}},\ s) = [\overleftrightarrow{\eta}(\hat{\mathbf{s}},\ s)]^T, \qquad (97)$$

$$\boldsymbol{h}(-\hat{\mathbf{s}},\ s) = \mathrm{diag}[1,\ -1][\boldsymbol{h}(\hat{\mathbf{s}},\ s)]^T\mathrm{diag}[1,\ -1]. \qquad (98)$$

F. Transfer Equation for the Coherent Field

We will now switch to quantities that have the dimension of monochromatic energy flux and can thus be measured by an optical device. We first define the coherency column vector of the coherent field according to

$$\boldsymbol{J}_c = \frac{1}{2}\sqrt{\frac{\varepsilon_1}{\mu_0}}\begin{bmatrix} E_{c\theta}E_{c\theta}^* \\ E_{c\theta}E_{c\phi}^* \\ E_{c\phi}E_{c\theta}^* \\ E_{c\phi}E_{c\phi}^* \end{bmatrix} \qquad (99)$$

and easily derive from Eqs. (92) and (94) the following transfer equation:

$$\frac{\mathrm{d}\boldsymbol{J}_c(\mathbf{r})}{\mathrm{d}s} = -n_0\langle \boldsymbol{K}^J(\hat{\mathbf{s}})\rangle \boldsymbol{J}_c(\mathbf{r}), \qquad (100)$$

where $\boldsymbol{K}^J$ is the coherency extinction matrix given by Eq. (30). The Stokes vector representation of this equation is obtained by use of the definition $\boldsymbol{I}_c = \boldsymbol{D}\boldsymbol{J}_c$ and Eq. (32):

$$\frac{\mathrm{d}\boldsymbol{I}_c(\mathbf{r})}{\mathrm{d}s} = -n_0\langle \boldsymbol{K}(\hat{\mathbf{s}})\rangle \boldsymbol{I}_c(\mathbf{r}), \qquad (101)$$

where $\boldsymbol{K}$ is the Stokes extinction matrix. Both $\boldsymbol{J}_c$ and $\boldsymbol{I}_c$ have the dimension of monochromatic energy flux. The formal solution of Eq. (101) can be written in the form

$$\boldsymbol{I}_c(\mathbf{r}) = \boldsymbol{H}[\hat{\mathbf{s}},\ s(\mathbf{r})]\boldsymbol{I}_c(\mathbf{r}_A), \qquad (102)$$

where

$$\boldsymbol{H}(\hat{\mathbf{s}},\ s) = \exp[-n_0\langle \boldsymbol{K}(\hat{\mathbf{s}})\rangle s] \qquad (103)$$

is the coherent transmission Stokes matrix. In view of Eq. (33), $\boldsymbol{H}$ obeys the following reciprocity relation:

$$\boldsymbol{H}(-\hat{\mathbf{s}},\ s) = \boldsymbol{\Delta}_3[\boldsymbol{H}(\hat{\mathbf{s}},\ s)]^T\boldsymbol{\Delta}_3. \qquad (104)$$

The interpretation of Eq. (102) is most transparent when the average extinction matrix is diagonal: $\langle \boldsymbol{K}(\hat{\mathbf{s}})\rangle = C_{\mathrm{ext}}\mathrm{diag}[1,\ 1,\ 1,\ 1]$, where C_{ext} is the ensemble-averaged extinction cross section per particle. This happens, for example, when the particles are spherically symmetric and are made of an optically isotropic material. In this case Eq. (102) becomes

$$\begin{aligned}\boldsymbol{I}_c(\mathbf{r}) &= \exp[-n_0 C_{\mathrm{ext}} s(\mathbf{r})]\boldsymbol{I}_c(\mathbf{r}_A) \\ &= \exp[-\alpha_{\mathrm{ext}} s(\mathbf{r})]\boldsymbol{I}_c(\mathbf{r}_A), \end{aligned} \qquad (105)$$

which means that the Stokes parameters of the coherent wave are exponentially attenuated as the wave travels through the discrete random medium. The attenuation rates for all four Stokes parameters are the same, which means that the polarization state of the wave does not change. Equation (105) is the standard Beer's law, in which $\alpha_{\mathrm{ext}} = n_0 C_{\mathrm{ext}} = n_0(C_{\mathrm{sca}} + C_{\mathrm{abs}})$ is the attenuation (or extinction) coefficient, C_{sca} is the scattering cross section, and C_{abs} is the absorption cross section. The attenuation is a combined result of scattering of the coherent field by particles in all directions and, possibly, absorption inside the particles and is an inalienable property of all the scattering media, even those composed of nonabsorbing particles with $C_{\mathrm{abs}} = 0$.

In general, the extinction matrix is not diagonal and can explicitly depend on the propagation direction. This occurs, for example, when the scattering medium is composed of nonrandomly oriented nonspherical particles. Then the coherent transmission matrix $\boldsymbol{H}$ in Eq. (103) can also have nonzero off-diagonal elements, thereby yielding different attenuation rates for different Stokes parameters and causing a change in the polarization state of the coherent wave as it propagates through the medium.

G. Dyadic Correlation Function

An important statistical characteristic of the multiple-scattering process is the so-called dyadic correlation function. It involves the total electric

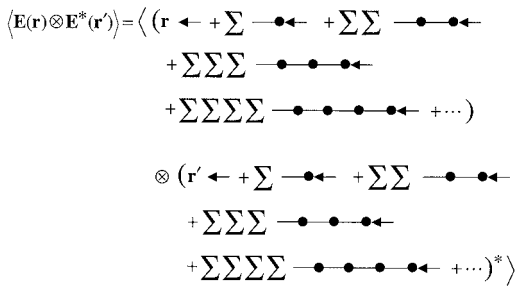

Fig. 9. Twersky representation of the dyadic correlation function.

fields at two points inside the medium and is defined as the ensemble average of the dyadic product $\mathbf{E}(\mathbf{r}) \otimes \mathbf{E}^*(\mathbf{r}')$. Obviously, the dyadic correlation function has the dimension of monochromatic energy flux.

Recalling the Twersky approximation (66) and Fig. 7(b), we conclude that the dyadic correlation function can be represented diagrammatically by Fig. 9. To classify different terms that enter the expanded expression inside the angular brackets on the right-hand side of this equation, we use the notation illustrated in Fig. 10(a). In this particular case, the upper and the lower scattering paths go through different particles. However, the two paths can involve one or more common particles, as shown in panels (b)–(d) by use of the dashed connectors. Furthermore, if the number of common particles is two or more, they can enter the upper and lower paths in the same order, as in panel (c), or in the reverse order, as in panel (d). Panel (e) shows a mixed diagram in which two common particles appear in the same order and two other common particles appear in reverse order. By nature of the Twersky approximation, neither the upper path nor the lower path can go through a particle more than once. Therefore, no particle can be the origin of more than one connector.

To sum and average all the diagrams that enter the expanded expression for the dyadic correlation function in Fig. 9 is a difficult problem that I will not try to attack. Instead, I will neglect all the diagrams with crossing connectors and will work with a truncated expansion that includes only the diagrams with vertical or no connectors. This approximation will allow us to sum and average large groups of diagrams

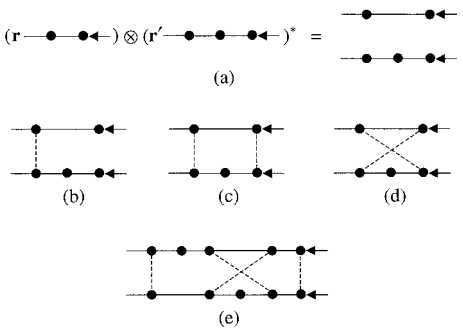

Fig. 10. Classification of terms that enter the Twersky expansion of the dyadic correlation function.

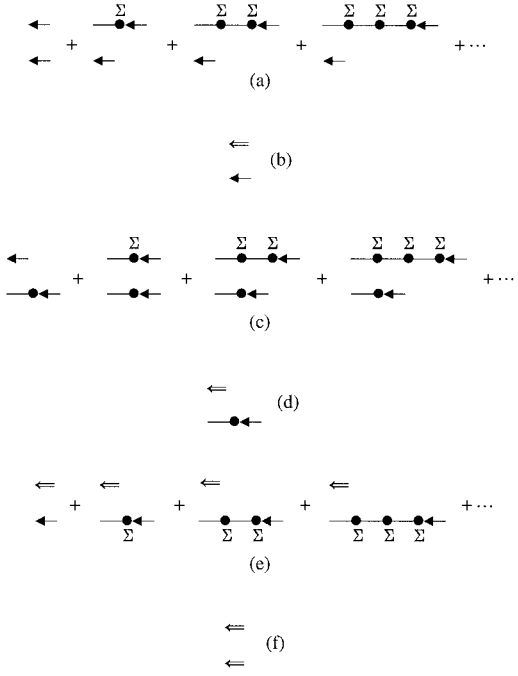

Fig. 11. Calculation of the total contribution of diagrams with no connectors.

independently and eventually derive the RTE. The consequences of neglecting the diagrams with crossing connectors will be discussed in Section 4.

Let us begin with diagrams that have no connectors. Since these diagrams do not involve common particles, the ensemble averaging of the upper and lower paths can be performed independently. Consider first the sum of the diagrams shown in Fig. 11(a), in which the Σ indicates both the summation over all appropriate particles and the statistical averaging over the particle states and positions. According to Subsection 3.E, summing the upper paths yields the coherent field at $\mathbf{r}_1$. This result can be represented by the diagram shown in Fig. 11(b), in which the $\Leftarrow$ denotes the coherent field. Similarly, summing the upper paths of the diagram shown in panel (c) gives, in the limit $N \to \infty$, the diagram shown in panel (d). Indeed, since one particle is already reserved for the lower path, the number of particles that contribute to the upper paths in panel (c) is $N - 1$. However, the difference between the sum of the upper paths in panel (c) and the coherent field at $\mathbf{r}_1$ vanishes as N tends to infinity. We can continue this process and eventually conclude that the total contribution of the diagrams with no connectors is given by the sum of the diagrams shown in panel (e). It is now clear that the final result can be represented by the diagram in panel (f), which means that the contribution of all the diagrams with no connectors to the dyadic correlation function is simply the dyadic product of the coherent fields at points $\mathbf{r}$ and $\mathbf{r}'$: $\mathbf{E}_c(\mathbf{r}) \otimes \mathbf{E}_c^*(\mathbf{r}')$.

All other diagrams that contribute to the dyadic correlation function have at least one vertical connector, as shown in Fig. 12(a). That part of the diagram

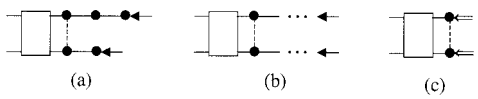

Fig. 12. Diagrams with one or more vertical connectors.

on the right-hand side of the rightmost connector will be called the tail, whereas the box represents collectively that part of the diagram on the left-hand side of the rightmost connector and can, in principle, be empty. The rightmost common particle and the box form the body of the diagram.

Let us first consider the group of diagrams with the same body but with different tails, as shown in Fig. 12(b). We can repeat the derivation of Subsection 3.E and verify that, in the limit $N \to \infty$, the sum of all the diagrams in Fig. 13(a) gives the diagram shown in Fig. 13(c). Indeed, let particle q be the rightmost connected particle and particle p be the rightmost particle on the left-hand side of particle q in the upper scattering paths of the diagrams shown in Fig. 13(a). The electric field created by particle q at the origin of particle p is represented by the sum of the diagrams on the left-hand side of Fig. 13(b) or, in expanded form, by

$$
\begin{aligned}
& G(R_{pq})\overleftrightarrow{A}(\hat{\mathbf{R}}_{pq}, \hat{\mathbf{s}}) \cdot \mathbf{E}_q^{\text{inc}} \\
& \quad + \frac{N-n}{N} n_0 G(R_{pq}) \int G(R_{qi})\overleftrightarrow{A}(\hat{\mathbf{R}}_{pq}, \hat{\mathbf{R}}_{qi}) \\
& \quad \cdot \langle \overleftrightarrow{A}(\hat{\mathbf{R}}_{qi}, \hat{\mathbf{s}}) \rangle \cdot \mathbf{E}_i^{\text{inc}} \mathrm{d}^3\mathbf{R}_i \\
& \quad + \frac{(N-n)(N-n-1)}{N^2} n_0{}^2 G(R_{pq}) \\
& \quad \times \int G(R_{qi})\overleftrightarrow{A}(\hat{\mathbf{R}}_{pq}, \hat{\mathbf{R}}_{qi}) \cdot \langle \overleftrightarrow{A}(\hat{\mathbf{R}}_{qi}, \hat{\mathbf{R}}_{ij}) \rangle \\
& \quad \cdot \langle \overleftrightarrow{A}(\hat{\mathbf{R}}_{ij}, \hat{\mathbf{s}}) \rangle \cdot \mathbf{E}_j^{\text{inc}} \mathrm{d}^3\mathbf{R}_i \mathrm{d}^3\mathbf{R}_j \\
& \quad + \cdots \underset{N \to \infty}{=} G(R_{pq})\overleftrightarrow{A}(\hat{\mathbf{R}}_{pq}, \hat{\mathbf{s}}) \cdot \mathbf{E}_c(\mathbf{R}_q),
\end{aligned}
$$

where n is the number of particles in the common body of the diagrams. The right-hand side of this equation was derived under the assumption that N is so large that all the factors of the type $(N-n)!/(N-n-k)!$ can be replaced by N^k. This result is summarized by the right-hand side of Fig. 13(b). Analogously, the sum of the diagrams in Fig. 13(d) is given by the diagram in Fig. 13(e), and so on. We can now sum up all the diagrams in Fig. 13(f) and obtain the diagram shown in Fig. 12(c). Thus the collective contribution to the dyadic correlation function of all the diagrams with the same body and all possible tails is equivalent to the contribution of a single diagram formed by the body alone, provided that the rightmost common particle is excited by the coherent field rather than by the external incident field. This important result allows us to cut off all the tails and consider only truncated diagrams of the type shown in Fig. 12(c).

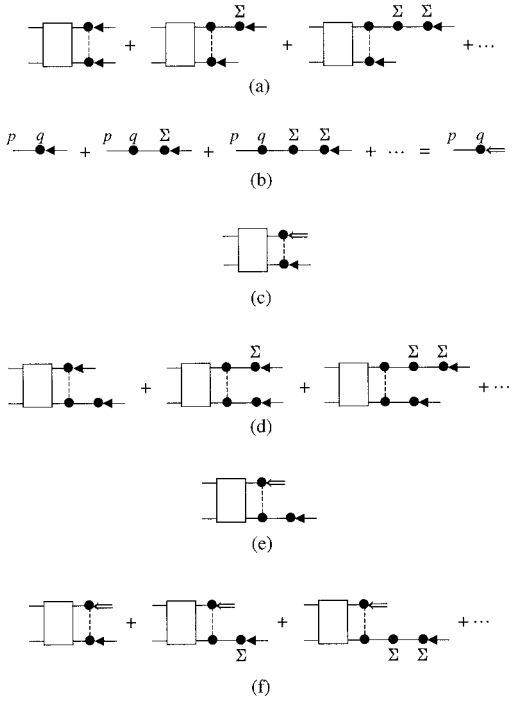

Fig. 13. Summation of the tails.

Thus the dyadic correlation function is equal to $\mathbf{E}_c(\mathbf{r}) \otimes \mathbf{E}_c{}^*(\mathbf{r}')$ plus the statistical average of the sum of all connected diagrams of the type illustrated by panels (a)–(c) of Fig. 14. The symbols $\cdots$ in these diagrams denote all possible combinations of unconnected particles. Let us, for example, consider the statistical average of the sum of all the diagrams of the kind shown in panel (c) with the same fixed shaded part. We thus must evaluate the left-hand side of the equation shown in panel (d), where, as before, the Σ indicates both the summation over all appropriate particles and the statistical averaging over the particle states and positions. Let particle r be the rightmost particle on the left-hand side of particle p in the upper scattering paths of the diagrams on the left-hand side of panel (d) and u be the leftmost particle on the right-hand side of particle q. The electric field created by particle p at the origin of particle r by all the diagrams shown on the left-hand side of panel (d) is given by the left-hand side of the equation shown diagrammatically in panel (e) and can be written in expanded form as

$$
\begin{aligned}
\mathbf{E}_r = {} & G(R_{rp})G(R_{pq})\overleftrightarrow{A}_p(\hat{\mathbf{R}}_{rp}, \hat{\mathbf{R}}_{pq}) \cdot \overleftrightarrow{A}_q(\hat{\mathbf{R}}_{pq}, \hat{\mathbf{R}}_{qu}) \cdot \mathbf{E}_q \\
& + \sum_i G(R_{rp}) \langle G(R_{pi})G(R_{iq})\overleftrightarrow{A}_p(\hat{\mathbf{R}}_{rp}, \hat{\mathbf{R}}_{pi}) \\
& \cdot \overleftrightarrow{A}_i(\hat{\mathbf{R}}_{pi}, \hat{\mathbf{R}}_{iq}) \cdot \overleftrightarrow{A}_q(\hat{\mathbf{R}}_{iq}, \hat{\mathbf{R}}_{qu}) \rangle \cdot \mathbf{E}_q \\
& + \sum_{ij} G(R_{rp}) \langle G(R_{pi})G(R_{ij})G(R_{jq})\overleftrightarrow{A}_p(\hat{\mathbf{R}}_{rp}, \hat{\mathbf{R}}_{pi}) \\
& \cdot \overleftrightarrow{A}_i(\hat{\mathbf{R}}_{pi}, \hat{\mathbf{R}}_{ij}) \cdot \overleftrightarrow{A}_j(\hat{\mathbf{R}}_{ij}, \hat{\mathbf{R}}_{jq}) \cdot \overleftrightarrow{A}_q(\hat{\mathbf{R}}_{jq}, \hat{\mathbf{R}}_{qu}) \rangle \\
& \cdot \mathbf{E}_q + \cdots, \qquad (106)
\end{aligned}
$$

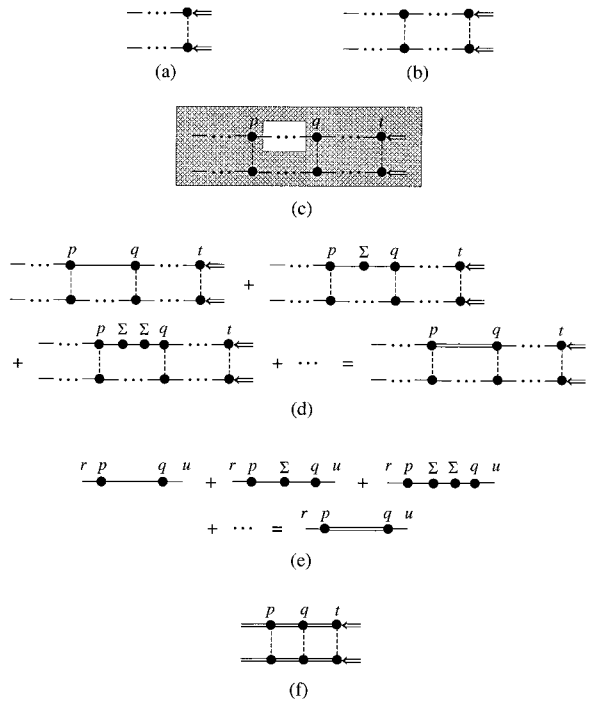

Fig. 14. Derivation of the ladder approximation for the dyadic correlation function.

where $\mathbf{E}_q$ is the field at the origin of particle q created by particle u and the summations and integrations are performed over all appropriate unconnected particles (see Fig. 15). In the limit $N \to \infty$, Eq. (106) takes the form

$$\begin{aligned}\mathbf{E}_r = {} & G(R_{rp})G(R_{pq})\overleftrightarrow{A}_p(\hat{\mathbf{R}}_{rp}, \hat{\mathbf{R}}_{pq}) \cdot \overleftrightarrow{A}_q(\hat{\mathbf{R}}_{pq}, \hat{\mathbf{R}}_{qu}) \cdot \mathbf{E}_q \\ & + n_0 G(R_{rp}) \int_V \mathrm{d}^3\mathbf{R}_i\, G(R_{pi})G(R_{iq})\overleftrightarrow{A}_p(\hat{\mathbf{R}}_{rp}, \hat{\mathbf{R}}_{pi}) \\ & \cdot \langle \overleftrightarrow{A}(\hat{\mathbf{R}}_{pi}, \hat{\mathbf{R}}_{iq})\rangle \cdot \overleftrightarrow{A}_q(\hat{\mathbf{R}}_{iq}, \hat{\mathbf{R}}_{qu}) \cdot \mathbf{E}_q \\ & + n_0{}^2 G(R_{rp}) \int_V \mathrm{d}^3\mathbf{R}_i \mathrm{d}^3\mathbf{R}_j\, G(R_{pi})G(R_{ij})G(R_{jq}) \\ & \times \overleftrightarrow{A}_p(\hat{\mathbf{R}}_{rp}, \hat{\mathbf{R}}_{pi}) \cdot \langle \overleftrightarrow{A}(\hat{\mathbf{R}}_{pi}, \hat{\mathbf{R}}_{ij})\rangle \\ & \cdot \langle \overleftrightarrow{A}(\hat{\mathbf{R}}_{ij}, \hat{\mathbf{R}}_{jq})\rangle \cdot \overleftrightarrow{A}_q(\hat{\mathbf{R}}_{jq}, \hat{\mathbf{R}}_{qu}) \cdot \mathbf{E}_q \\ & + \cdots. \end{aligned} \tag{107}$$

Let us consider the first integral of Eq. (107) and denote it $\mathbf{I}_1$. Since the factor $\exp[\mathrm{i}k_1(R_{pi} + R_{iq})]$ is a rapidly oscillating function of $\mathbf{R}_i$, the contribution of a major part of V to $\mathbf{I}_1$ can be expected to zero out. The only exception is the small region around the straight line that connects particles q and p, where $\exp[\mathrm{i}k_1(R_{pi} + R_{iq})]$ is almost constant. Therefore, we can evaluate $\mathbf{I}_1$ using the method of stationary phase (see, e.g., Appendix 14B of Ref. 20). By use of the laboratory coordinate system with the origin at O, as shown in Fig. 15, $\mathbf{I}_1$ can be rewritten in the form

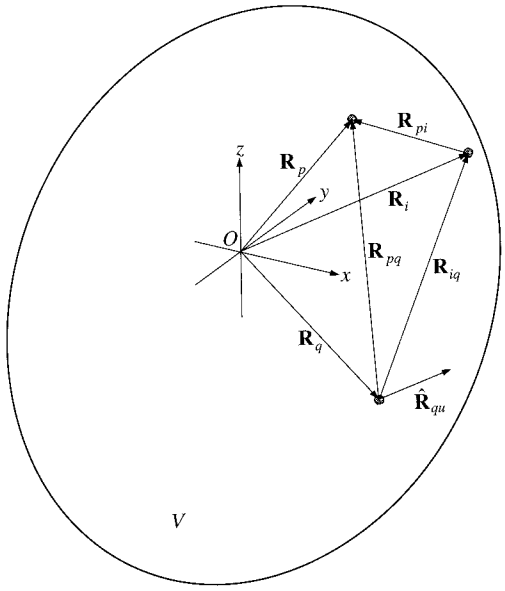

Fig. 15. Calculation of the integrals in Eq. (107).

$$\begin{aligned}\mathbf{I}_1 = {} & n_0 G(R_{rp}) \int_{-\infty}^{+\infty} \mathrm{d}x_i \int_{-\infty}^{+\infty} \mathrm{d}y_i \int \mathrm{d}z_i \\ & \times \frac{\exp[\mathrm{i}k_1(R_{pi} + R_{iq})]}{R_{pi}R_{iq}} \overleftrightarrow{A}_p(\hat{\mathbf{R}}_{rp}, \hat{\mathbf{R}}_{pi}) \\ & \cdot \langle \overleftrightarrow{A}(\hat{\mathbf{R}}_{pi}, \hat{\mathbf{R}}_{iq})\rangle \cdot \overleftrightarrow{A}_q(\hat{\mathbf{R}}_{iq}, \hat{\mathbf{R}}_{qu}) \cdot \mathbf{E}_q, \end{aligned} \tag{108}$$

where we have set infinite integration limits for x_i and y_i owing to the fact that only a small part of V contributes to $\mathbf{I}_1$. The integral over z_i can be subdivided into three integrals covering the regions with $z_i < z_q$, $z_q < z_i < z_p$, and $z_p < z_i$. The first and third integrals involve rapidly oscillating functions of z_i and vanish, so that only the interval $z_q < z_i < z_p$ gives a nonzero contribution. We can now use Eq. (14–53) of Ref. 20 to derive

$$\begin{aligned}\mathbf{I}_1 = {} & G(R_{rp}) \frac{\exp(\mathrm{i}k_1 R_{pq})}{R_{pq}} \frac{\mathrm{i}2\pi n_0 R_{pq}}{k_1} \overleftrightarrow{A}_p(\hat{\mathbf{R}}_{rp}, \hat{\mathbf{R}}_{pq}) \\ & \cdot \langle \overleftrightarrow{A}(\hat{\mathbf{R}}_{pq}, \hat{\mathbf{R}}_{pq})\rangle \cdot \overleftrightarrow{A}_q(\hat{\mathbf{R}}_{pq}, \hat{\mathbf{R}}_{qu}) \cdot \mathbf{E}_q. \end{aligned} \tag{109}$$

The other integrals on the right-hand side of Eq. (107) are computed analogously. The final result is

$$\begin{aligned}\mathbf{E}_r = {} & G(R_{rp})\overleftrightarrow{A}_p(\hat{\mathbf{R}}_{rp}, \hat{\mathbf{R}}_{pq}) \cdot \frac{\overleftrightarrow{\eta}(\hat{\mathbf{R}}_{pq}, R_{pq})}{R_{pq}} \\ & \cdot \overleftrightarrow{A}_q(\hat{\mathbf{R}}_{pq}, \hat{\mathbf{R}}_{qu}) \cdot \mathbf{E}_q, \end{aligned} \tag{110}$$

where the coherent transmission dyad $\overleftrightarrow{\eta}$ is given by Eq. (89). This equation is similar to Eq. (87) for the coherent field and describes the coherent propagation

of the wave scattered by particle q toward particle p through the scattering medium. The presence of other particles on the line of sight causes attenuation and, potentially, a change in polarization state of the wave. The obvious difference from Eq. (87) is the factor $1/R_{pq}$, which is a reminder that the wave scattered by a particle is spherical, whereas the coherent field is a plane wave.

Equation (110) can be summarized by the diagram on the right-hand side of Fig. 14(e). The double line rather than a single line indicates that the scalar factor $\exp[ik_1 R_{pq}]/R_{pq}$ has been replaced by the dyadic factor $\exp[i\overleftrightarrow{\kappa}(\hat{\mathbf{R}}_{pq})R_{pq}]/R_{pq}$. It is now clear that the total contribution of all the diagrams with three fixed common particles t, q, and p to the dyadic correlation function can be represented by the diagram in Fig. 14(f) or, in expanded form, by the formula

$$
\begin{aligned}
&\left[\frac{\overleftrightarrow{\eta}(\hat{\mathbf{R}}_{1p}, R_{1p})}{R_{1p}} \cdot \overleftrightarrow{A}_p(\hat{\mathbf{R}}_{1p}, \hat{\mathbf{R}}_{pq})\right.\\
&\quad \cdot \frac{\overleftrightarrow{\eta}(\hat{\mathbf{R}}_{pq}, R_{pq})}{R_{pq}} \cdot \overleftrightarrow{A}_q(\hat{\mathbf{R}}_{pq}, \hat{\mathbf{R}}_{qt})\\
&\quad \left. \cdot \frac{\overleftrightarrow{\eta}(\hat{\mathbf{R}}_{qt}, R_{qt})}{R_{qt}} \cdot \overleftrightarrow{A}_t(\hat{\mathbf{R}}_{qt}, \hat{\mathbf{s}}) \cdot \mathbf{E}_c(\mathbf{R}_t)\right]\\
&\otimes \left[\frac{\overleftrightarrow{\eta}(\hat{\mathbf{R}}_{2p}, R_{2p})}{R_{2p}} \cdot \overleftrightarrow{A}_p(\hat{\mathbf{R}}_{2p}, \hat{\mathbf{R}}_{pq})\right.\\
&\quad \cdot \frac{\overleftrightarrow{\eta}(\hat{\mathbf{R}}_{pq}, R_{pq})}{R_{pq}} \cdot \overleftrightarrow{A}_q(\hat{\mathbf{R}}_{pq}, \hat{\mathbf{R}}_{qt})\\
&\quad \left. \cdot \frac{\overleftrightarrow{\eta}(\hat{\mathbf{R}}_{qt}, R_{qt})}{R_{qt}} \cdot \overleftrightarrow{A}_t(\hat{\mathbf{R}}_{qt}, \hat{\mathbf{s}}) \cdot \mathbf{E}_c(\mathbf{R}_t)\right]^*,
\end{aligned}
$$

where subscripts 1 and 2 refer to observation points $\mathbf{r}_1$ and $\mathbf{r}_2$, respectively.

After we have neglected all the diagrams with crossing connectors, computed the contribution of all the diagrams with no connectors, and figured out how to calculate the contributions from various diagrams with one or more vertical connectors, we are perfectly positioned to complete the derivation of the dyadic correlation function. The final result is shown in Fig. 16, where the Σ has its usual meaning. Owing to their appearance, the diagrams on the right-hand side of this equation are called ladder diagrams. Therefore, this entire formula can be called the ladder approximation for the dyadic correlation function.

H. Integral Equation for the Specific Coherency Dyad

The coherency dyad $\overleftrightarrow{C}(\mathbf{r})$ is defined as $\overleftrightarrow{C}(\mathbf{r}) = \langle \mathbf{E}(\mathbf{r}) \otimes \mathbf{E}^*(\mathbf{r}) \rangle$. The expanded form of the ladder approximation for the coherency dyad follows from Figs. 16 and 17:

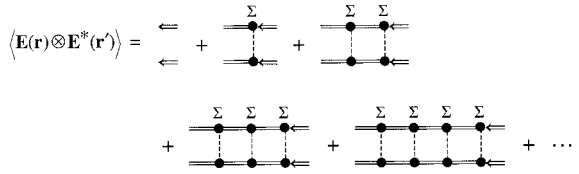

Fig. 16. Ladder approximation for the dyadic correlation function.

$$
\begin{aligned}
\overleftrightarrow{C}(\mathbf{r}) = \overleftrightarrow{C}_c(\mathbf{r}) &+ n_0 \int \mathrm{d}^3\mathbf{R}_1 \mathrm{d}\xi_1 \frac{\overleftrightarrow{\eta}(\hat{\mathbf{r}}_1, r_1)}{r_1} \cdot \overleftrightarrow{A}_1(\hat{\mathbf{r}}_1, \hat{\mathbf{s}})\\
&\cdot \overleftrightarrow{C}_c(\mathbf{R}_1) \cdot \overleftrightarrow{A}_1^{T^*}(\hat{\mathbf{r}}_1, \hat{\mathbf{s}}) \cdot \frac{\overleftrightarrow{\eta}^{T^*}(\hat{\mathbf{r}}_1, r_1)}{r_1}\\
&+ n_0^2 \int \mathrm{d}^3\mathbf{R}_1 \mathrm{d}\xi_1 \int \mathrm{d}^3\mathbf{R}_2 \mathrm{d}\xi_2 \frac{\overleftrightarrow{\eta}(\hat{\mathbf{r}}_1, r_1)}{r_1}\\
&\cdot \overleftrightarrow{A}_1(\hat{\mathbf{r}}_1, \hat{\mathbf{R}}_{12}) \cdot \frac{\overleftrightarrow{\eta}(\hat{\mathbf{R}}_{12}, R_{12})}{R_{12}} \cdot \overleftrightarrow{A}_2(\hat{\mathbf{R}}_{12}, \hat{\mathbf{s}})\\
&\cdot \overleftrightarrow{C}_c(\mathbf{R}_2) \cdot \overleftrightarrow{A}_2^{T^*}(\hat{\mathbf{R}}_{12}, \hat{\mathbf{s}}) \cdot \frac{\overleftrightarrow{\eta}^{T^*}(\hat{\mathbf{R}}_{12}, R_{12})}{R_{12}}\\
&\cdot \overleftrightarrow{A}_1^{T^*}(\hat{\mathbf{r}}_1, \hat{\mathbf{R}}_{12}) \cdot \frac{\overleftrightarrow{\eta}^{T^*}(\hat{\mathbf{r}}_1, r_1)}{r_1} + \cdots, \qquad (111)
\end{aligned}
$$

where $\overleftrightarrow{C}_c(\mathbf{r}) = \mathbf{E}_c(\mathbf{r}) \otimes \mathbf{E}_c^*(\mathbf{r})$ is the coherent part of the coherency dyad, and we have taken into account

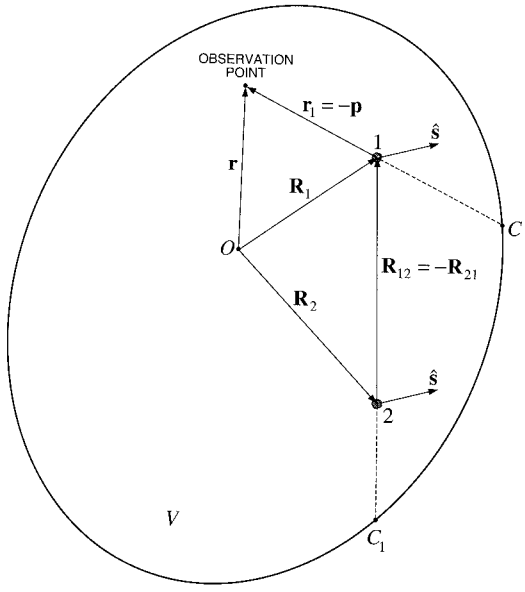

Fig. 17. Geometry showing the quantities used in Eq. (111).

that $(\overleftrightarrow{B}\cdot\mathbf{E})\otimes(\overleftrightarrow{B}^{*}\cdot\mathbf{E}^{*})=\overleftrightarrow{B}\cdot(\mathbf{E}\otimes\mathbf{E}^{*})\cdot\overleftrightarrow{B}^{T^{*}}$ and $(\overleftrightarrow{B}\cdot\overleftrightarrow{D})^{T}=\overleftrightarrow{D}^{T}\cdot\overleftrightarrow{B}^{T}$.

It is convenient to integrate over all positions of particle 1 by use of a local coordinate system with its origin at the observation point, integrate over all positions of particle 2 by use of a local coordinate system with its origin at the origin of particle 1, etc. Using the notation introduced in Fig. 17 and taking into account that $\mathrm{d}^{3}\mathbf{p}=r_{1}^{2}\mathrm{d}p\mathrm{d}\hat{\mathbf{p}}$, $\mathrm{d}^{3}\mathbf{R}_{21}=R_{12}^{2}\mathrm{d}R_{21}\mathrm{d}\hat{\mathbf{R}}_{21}$, and so on, from Eq. (111) we get

$$\overleftrightarrow{C}(\mathbf{r})=\int_{4\pi}\mathrm{d}\hat{\mathbf{p}}\,\overleftrightarrow{\Sigma}(\mathbf{r},\,-\hat{\mathbf{p}}),\tag{112}$$

where $\overleftrightarrow{\Sigma}(\mathbf{r},\,-\hat{\mathbf{p}})$ is the so-called specific coherency dyad defined by

$$\begin{aligned}\overleftrightarrow{\Sigma}(\mathbf{r},\,-\hat{\mathbf{p}})&=\delta(\hat{\mathbf{p}}+\hat{\mathbf{s}})\overleftrightarrow{C}_{c}(\mathbf{r})\\&+n_{0}\int\mathrm{d}p\mathrm{d}\xi_{1}\overleftrightarrow{\eta}(-\hat{\mathbf{p}},p)\cdot\overleftrightarrow{A}_{1}(-\hat{\mathbf{p}},\hat{\mathbf{s}})\\&\cdot\overleftrightarrow{C}_{c}(\mathbf{r}+\mathbf{p})\cdot\overleftrightarrow{A}_{1}^{T^{*}}(-\hat{\mathbf{p}},\hat{\mathbf{s}})\\&\cdot\overleftrightarrow{\eta}^{T^{*}}(-\hat{\mathbf{p}},p)+n_{0}^{2}\int\mathrm{d}p\mathrm{d}\xi_{1}\\&\times\int\mathrm{d}R_{21}\mathrm{d}\hat{\mathbf{R}}_{21}\mathrm{d}\xi_{2}\overleftrightarrow{\eta}(-\hat{\mathbf{p}},p)\\&\cdot\overleftrightarrow{A}_{1}(-\hat{\mathbf{p}},\,-\hat{\mathbf{R}}_{21})\cdot\overleftrightarrow{\eta}(-\hat{\mathbf{R}}_{21},R_{21})\\&\cdot\overleftrightarrow{A}_{2}(-\hat{\mathbf{R}}_{21},\hat{\mathbf{s}})\cdot\overleftrightarrow{C}_{c}(\mathbf{r}+\mathbf{p}+\mathbf{R}_{21})\\&\cdot\overleftrightarrow{A}_{2}^{T^{*}}(-\hat{\mathbf{R}}_{21},\hat{\mathbf{s}})\cdot\overleftrightarrow{\eta}^{T^{*}}(-\hat{\mathbf{R}}_{21},R_{21})\\&\cdot\overleftrightarrow{A}_{1}^{T^{*}}(-\hat{\mathbf{p}},\,-\hat{\mathbf{R}}_{21})\cdot\overleftrightarrow{\eta}^{T^{*}}(-\hat{\mathbf{p}},p)+\cdots.\end{aligned}\tag{113}$$

Note that p ranges from zero at the observation point to the corresponding value at the point where the straight line in the $\hat{\mathbf{p}}$ direction crosses the boundary of the medium (point C in Fig. 17), R_{21} ranges from zero at the origin of particle 1 to the corresponding value at point C_1, etc. Importantly, the specific coherency dyad has the dimension of specific intensity ($\mathrm{Wm}^{-2}\,\mathrm{sr}^{-1}$) rather than that of monochromatic energy flux (Wm^{-2}).

It can be easily verified that $\overleftrightarrow{\Sigma}$ satisfies the following integral equation:

$$\begin{aligned}\overleftrightarrow{\Sigma}(\mathbf{r},\,-\hat{\mathbf{p}})&=\delta(\hat{\mathbf{p}}+\hat{\mathbf{s}})\overleftrightarrow{C}_{c}(\mathbf{r})\\&+n_{0}\int\mathrm{d}p\mathrm{d}\xi\mathrm{d}\hat{\mathbf{p}}'\overleftrightarrow{\eta}(-\hat{\mathbf{p}},p)\\&\cdot\overleftrightarrow{A}(-\hat{\mathbf{p}},\,-\hat{\mathbf{p}}')\cdot\overleftrightarrow{\Sigma}(\mathbf{r}+\mathbf{p},\,-\hat{\mathbf{p}}')\\&\cdot\overleftrightarrow{A}^{T^{*}}(-\hat{\mathbf{p}},\,-\hat{\mathbf{p}}')\cdot\overleftrightarrow{\eta}^{T^{*}}(-\hat{\mathbf{p}},p).\end{aligned}\tag{114}$$

Indeed, using $\delta(\hat{\mathbf{p}}+\hat{\mathbf{s}})\overleftrightarrow{C}_{c}(\mathbf{r})$ as an initial approximation for $\overleftrightarrow{\Sigma}(\mathbf{r},\,-\hat{\mathbf{p}})$, we can substitute it into the integral on the right-hand side of Eq. (114) and obtain an improved approximation. By continuing this iterative process, we arrive at Eq. (113), which is simply the Neumann order-of-scattering expansion of the specific coherency dyad with the coherent field serving as the source of multiple scattering.

The interpretation of Eq. (114) is transparent: the specific coherency dyad for direction $-\hat{\mathbf{p}}$ at point $\mathbf{r}$ consists of a coherent part and an incoherent part. The latter is a cumulative contribution of all particles located along the straight line in the $\hat{\mathbf{p}}$ direction and scattering radiation coming from all directions $-\hat{\mathbf{p}}'$ into direction $-\hat{\mathbf{p}}$.

I. Radiative Transfer Equation for the Specific Coherency Dyad

To derive the differential form of Eq. (114), we introduce a q axis as shown in Fig. 18. This axis originates at point C and goes through the observation point in the direction of the unit vector $\hat{\mathbf{q}}=-\hat{\mathbf{p}}$ (see Fig. 17). We can now rewrite Eq. (114) as

$$\begin{aligned}\overleftrightarrow{\Sigma}(Q,\,\hat{\mathbf{q}})&=\delta(\hat{\mathbf{q}}-\hat{\mathbf{s}})\overleftrightarrow{C}_{c}(Q)\\&+n_{0}\int_{0}^{Q}\mathrm{d}q\int\mathrm{d}\xi\int_{4\pi}\mathrm{d}\hat{\mathbf{q}}'\overleftrightarrow{\eta}(\mathbf{q},Q-a)\\&\cdot\overleftrightarrow{A}(\hat{\mathbf{q}},\hat{\mathbf{q}}')\cdot\overleftrightarrow{\Sigma}(q,\hat{\mathbf{q}}')\\&\cdot\overleftrightarrow{A}^{T^{*}}(\hat{\mathbf{q}},\hat{\mathbf{q}}')\cdot\overleftrightarrow{\eta}^{T^{*}}(\hat{\mathbf{q}},Q-q).\end{aligned}\tag{115}$$

The diffuse specific coherency dyad is defined as the difference between the full specific coherency dyad and its coherent component: $\overleftrightarrow{\Sigma}_{\mathrm{d}}(Q,\hat{\mathbf{q}})=\overleftrightarrow{\Sigma}(Q,\hat{\mathbf{q}})-\delta(\hat{\mathbf{q}}-\hat{\mathbf{s}})\overleftrightarrow{C}_{c}(Q)$. The integral equation for $\overleftrightarrow{\Sigma}_{\mathrm{d}}(Q,\hat{\mathbf{q}})$ follows from Eq. (115):

$$\begin{aligned}\overleftrightarrow{\Sigma}_{\mathrm{d}}(Q,\,\hat{\mathbf{q}})&=n_{0}\int_{0}^{Q}\mathrm{d}q\int\mathrm{d}\xi\overleftrightarrow{\eta}(\hat{\mathbf{q}},Q-q)\\&\cdot\overleftrightarrow{A}(\hat{\mathbf{q}},\hat{\mathbf{s}})\overleftrightarrow{C}_{c}(q)\\&\cdot\overleftrightarrow{A}^{T^{*}}(\hat{\mathbf{q}},\hat{\mathbf{s}})\cdot\overleftrightarrow{\eta}^{T^{*}}(\hat{\mathbf{q}},Q-q)\\&+n_{0}\int_{0}^{Q}\mathrm{d}q\int\mathrm{d}\xi\int_{4\pi}\mathrm{d}\hat{\mathbf{q}}'\overleftrightarrow{\eta}(\hat{\mathbf{q}},Q-q)\\&\cdot\overleftrightarrow{A}(\hat{\mathbf{q}},\hat{\mathbf{q}}')\cdot\overleftrightarrow{\Sigma}_{\mathrm{d}}(q,\hat{\mathbf{q}}')\\&\cdot\overleftrightarrow{A}^{T^{*}}(\hat{\mathbf{q}},\hat{\mathbf{q}}')\cdot\overleftrightarrow{\eta}^{T^{*}}(\hat{\mathbf{q}},Q-q).\end{aligned}\tag{116}$$

Differentiating both sides of Eq. (116) using the Leibnitz rule finally yields

$$\frac{\mathrm{d}\overleftrightarrow{\Sigma}_{\mathrm{d}}(Q,\hat{\mathbf{q}})}{\mathrm{d}Q} = \mathrm{i}\overleftrightarrow{\kappa}(\hat{\mathbf{q}})\cdot\overleftrightarrow{\Sigma}_{\mathrm{d}}(Q,\hat{\mathbf{q}}) - \mathrm{i}\overleftrightarrow{\Sigma}_{\mathrm{d}}(Q,\hat{\mathbf{q}})\cdot\overleftrightarrow{\kappa}^{T^*}(\hat{\mathbf{q}}) + n_0\int \mathrm{d}\xi \int_{4\pi} \mathrm{d}\hat{\mathbf{q}}'\overleftrightarrow{A}(\hat{\mathbf{q}},\hat{\mathbf{q}}')\cdot\overleftrightarrow{\Sigma}_{\mathrm{d}}(Q,\hat{\mathbf{q}}')\cdot\overleftrightarrow{A}^{T^*}(\hat{\mathbf{q}},\hat{\mathbf{q}}') + n_0\int \mathrm{d}\xi\overleftrightarrow{A}(\hat{\mathbf{q}},\hat{\mathbf{s}})\cdot\overleftrightarrow{C}_c(Q)\cdot\overleftrightarrow{A}^{T^*}(\hat{\mathbf{q}},\hat{\mathbf{s}}). \quad (117)$$

For further use, it is more convenient to rewrite Eq. (117) in the following form:

$$\frac{\mathrm{d}\overleftrightarrow{\Sigma}_{\mathrm{d}}(\mathbf{r},\hat{\mathbf{q}})}{\mathrm{d}q} = \mathrm{i}\overleftrightarrow{\kappa}(\hat{\mathbf{q}})\cdot\overleftrightarrow{\Sigma}_{\mathrm{d}}(\mathbf{r},\hat{\mathbf{q}}) - \mathrm{i}\overleftrightarrow{\Sigma}_{\mathrm{d}}(\mathbf{r},\hat{\mathbf{q}})\cdot\overleftrightarrow{\kappa}^{T^*}(\hat{\mathbf{q}}) + n_0\int \mathrm{d}\xi \int_{4\pi} \mathrm{d}\hat{\mathbf{q}}'\overleftrightarrow{A}(\hat{\mathbf{q}},\hat{\mathbf{q}}')\cdot\overleftrightarrow{\Sigma}_{\mathrm{d}}(\mathbf{r},\hat{\mathbf{q}}')\cdot\overleftrightarrow{A}^{T^*}(\hat{\mathbf{q}},\hat{\mathbf{q}}') + n_0\int \mathrm{d}\xi\overleftrightarrow{A}(\hat{\mathbf{q}},\hat{\mathbf{s}})\cdot\overleftrightarrow{C}_c(\mathbf{r})\cdot\overleftrightarrow{A}^{T^*}(\hat{\mathbf{q}},\hat{\mathbf{s}}), \quad (118)$$

where $\overleftrightarrow{\Sigma}_{\mathrm{d}}(\mathbf{r},\hat{\mathbf{q}}) = \overleftrightarrow{\Sigma}(\mathbf{r},\hat{\mathbf{q}}) - \delta(\hat{\mathbf{q}}-\hat{\mathbf{s}})\overleftrightarrow{C}_c(\mathbf{r})$ and the path-length element $\mathrm{d}q$ is measured along the unit vector $\hat{\mathbf{q}}$. Equation (118) is the integrodifferential RTE for the diffuse specific coherency dyad.

J. Radiative Transfer Equation for the Specific Intensity Vector

It follows from Eq. (116) that $\hat{\mathbf{q}}\cdot\overleftrightarrow{\Sigma}_{\mathrm{d}}(\mathbf{r},\hat{\mathbf{q}}) = \overleftrightarrow{\Sigma}_{\mathrm{d}}(\mathbf{r},\hat{\mathbf{q}})\cdot\hat{\mathbf{q}} = 0$. This allows us to introduce the 2×2 diffuse specific coherency matrix $\tilde{\boldsymbol{\rho}}_{\mathrm{d}}$ using the local coordinate system with its origin at the observation point and orientation identical to that of the laboratory coordinate system:

$$\tilde{\boldsymbol{\rho}}_{\mathrm{d}}(\mathbf{r},\hat{\mathbf{q}}) = \frac{1}{2}\sqrt{\frac{\varepsilon_1}{\mu_0}}\begin{bmatrix} \hat{\boldsymbol{\theta}}(\hat{\mathbf{q}})\cdot\overleftrightarrow{\Sigma}_{\mathrm{d}}(\mathbf{r},\hat{\mathbf{q}})\cdot\hat{\boldsymbol{\theta}}(\hat{\mathbf{q}}) & \hat{\boldsymbol{\theta}}(\hat{\mathbf{q}})\cdot\overleftrightarrow{\Sigma}_{\mathrm{d}}(\mathbf{r},\hat{\mathbf{q}})\cdot\hat{\boldsymbol{\phi}}(\hat{\mathbf{q}}) \\ \hat{\boldsymbol{\phi}}(\hat{\mathbf{q}})\cdot\overleftrightarrow{\Sigma}_{\mathrm{d}}(\mathbf{r},\hat{\mathbf{q}})\cdot\hat{\boldsymbol{\theta}}(\hat{\mathbf{q}}) & \hat{\boldsymbol{\phi}}(\hat{\mathbf{q}})\cdot\overleftrightarrow{\Sigma}_{\mathrm{d}}(\mathbf{r},\hat{\mathbf{q}})\cdot\hat{\boldsymbol{\phi}}(\hat{\mathbf{q}}) \end{bmatrix}. \quad (119)$$

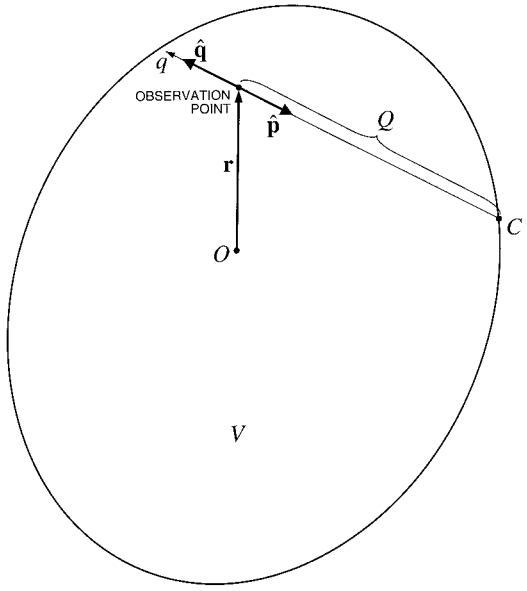

Fig. 18. Geometry showing the quantities used in the derivation of the VRTE.

We can then rewrite Eq. (118) in the form of the RTE for the diffuse specific coherency matrix:

$$\frac{\mathrm{d}\tilde{\boldsymbol{\rho}}_{\mathrm{d}}(\mathbf{r},\hat{\mathbf{q}})}{\mathrm{d}q} = \mathrm{i}\boldsymbol{k}(\hat{\mathbf{q}})\tilde{\boldsymbol{\rho}}_{\mathrm{d}}(\mathbf{r},\hat{\mathbf{q}}) - \mathrm{i}\tilde{\boldsymbol{\rho}}_{\mathrm{d}}(\mathbf{r},\hat{\mathbf{q}})\boldsymbol{k}^{T^*}(\hat{\mathbf{q}}) + n_0\int \mathrm{d}\xi \int_{4\pi} \mathrm{d}\hat{\mathbf{q}}'\boldsymbol{S}(\hat{\mathbf{q}},\hat{\mathbf{q}}')\tilde{\boldsymbol{\rho}}_{\mathrm{d}}(\mathbf{r},\hat{\mathbf{q}}')\boldsymbol{S}^{T^*}(\hat{\mathbf{q}},\hat{\mathbf{q}}') + n_0\int \mathrm{d}\xi\boldsymbol{S}(\hat{\mathbf{q}},\hat{\mathbf{s}})\boldsymbol{\rho}_c(\mathbf{r})\boldsymbol{S}^{T^*}(\hat{\mathbf{q}},\hat{\mathbf{s}}), \quad (120)$$

where $\boldsymbol{S}$ is the amplitude matrix, $\boldsymbol{k}$ is the matrix propagation constant given by Eq. (93), and

$$\boldsymbol{\rho}_c(\mathbf{r}) = \frac{1}{2}\times\sqrt{\frac{\varepsilon_1}{\mu_0}}\begin{bmatrix} \hat{\boldsymbol{\theta}}(\hat{\mathbf{s}})\cdot\overleftrightarrow{C}_c(\mathbf{r})\cdot\hat{\boldsymbol{\theta}}(\hat{\mathbf{s}}) & \hat{\boldsymbol{\theta}}(\hat{\mathbf{s}})\cdot\overleftrightarrow{C}_c(\mathbf{r})\cdot\hat{\boldsymbol{\phi}}(\hat{\mathbf{s}}) \\ \hat{\boldsymbol{\phi}}(\hat{\mathbf{s}})\cdot\overleftrightarrow{C}_c(\mathbf{r})\cdot\hat{\boldsymbol{\theta}}(\hat{\mathbf{s}}) & \hat{\boldsymbol{\phi}}(\hat{\mathbf{s}})\cdot\overleftrightarrow{C}_c(\mathbf{r})\cdot\hat{\boldsymbol{\phi}}(\hat{\mathbf{s}}) \end{bmatrix}. \quad (121)$$

The next obvious step is to introduce the corresponding coherency column vectors $\tilde{\boldsymbol{J}}_{\mathrm{d}}$ and $\boldsymbol{J}_c$:

$$\tilde{\boldsymbol{J}}_{\mathrm{d}}(\mathbf{r},\hat{\mathbf{q}}) = \begin{bmatrix} \tilde{\rho}_{\mathrm{d}11}(\mathbf{r},\hat{\mathbf{q}}) \\ \tilde{\rho}_{\mathrm{d}12}(\mathbf{r},\hat{\mathbf{q}}) \\ \tilde{\rho}_{\mathrm{d}21}(\mathbf{r},\hat{\mathbf{q}}) \\ \tilde{\rho}_{\mathrm{d}22}(\mathbf{r},\hat{\mathbf{q}}) \end{bmatrix}, \qquad \boldsymbol{J}_c(\mathbf{r}) = \begin{bmatrix} \rho_{c11}(\mathbf{r}) \\ \rho_{c12}(\mathbf{r}) \\ \rho_{c21}(\mathbf{r}) \\ \rho_{c22}(\mathbf{r}) \end{bmatrix} \quad (122)$$

[see Eq. (99)]. After lengthy but simple algebraic manipulations, we get

$$\frac{\mathrm{d}\tilde{\boldsymbol{J}}_{\mathrm{d}}(\mathbf{r},\,\hat{\mathbf{q}})}{\mathrm{d}q} = -n_0\langle \boldsymbol{K}^J(\hat{\mathbf{q}})\rangle\tilde{\boldsymbol{J}}_{\mathrm{d}}(\mathbf{r},\,\hat{\mathbf{q}}) + n_0\int_{4\pi}\mathrm{d}\hat{\mathbf{q}}'\langle \boldsymbol{Z}^J(\hat{\mathbf{q}},\,\hat{\mathbf{q}}')\rangle\tilde{\boldsymbol{J}}_{\mathrm{d}}(\mathbf{r},\,\hat{\mathbf{q}}') + n_0\langle \boldsymbol{Z}^J(\hat{\mathbf{q}},\,\hat{\mathbf{s}})\rangle\boldsymbol{J}_c(\mathbf{r}), \tag{123}$$

where $\langle \boldsymbol{K}^J(\hat{\mathbf{q}})\rangle$ is the coherency extinction matrix averaged over the particle states and $\langle \boldsymbol{Z}^J(\hat{\mathbf{q}},\,\hat{\mathbf{q}}')\rangle$ is the ensemble average of the coherency phase matrix given by Eq. (25). The column vector $\boldsymbol{J}_c(\mathbf{r})$ satisfies the transfer equation (100).

The final step in the derivation of the VRTE is to define the diffuse specific intensity column vector, $\tilde{\boldsymbol{I}}_{\mathrm{d}}(\mathbf{r},\,\hat{\mathbf{q}}) = \boldsymbol{D}\tilde{\boldsymbol{J}}_{\mathrm{d}}(\mathbf{r},\,\hat{\mathbf{q}})$, and the coherent Stokes column vector, $\boldsymbol{I}_{\mathrm{c}}(\mathbf{r}) = \boldsymbol{D}\boldsymbol{J}_{\mathrm{c}}(\mathbf{r})$, and rewrite Eq. (123) in the form

$$\frac{\mathrm{d}\tilde{\boldsymbol{I}}_{\mathrm{d}}(\mathbf{r},\,\hat{\mathbf{q}})}{\mathrm{d}q} = -n_0\langle \boldsymbol{K}(\hat{\mathbf{q}})\rangle\tilde{\boldsymbol{I}}_{\mathrm{d}}(\mathbf{r},\,\hat{\mathbf{q}}) + n_0\int_{4\pi}\mathrm{d}\hat{\mathbf{q}}'\langle \boldsymbol{Z}(\hat{\mathbf{q}},\,\hat{\mathbf{q}}')\rangle\tilde{\boldsymbol{I}}_{\mathrm{d}}(\mathbf{r},\,\hat{\mathbf{q}}') + n_0\langle \boldsymbol{Z}(\hat{\mathbf{q}},\,\hat{\mathbf{s}})\rangle\boldsymbol{I}_c(\mathbf{r}), \tag{124}$$

where $\langle \boldsymbol{K}(\hat{\mathbf{q}})\rangle$ is the ensemble average of the Stokes extinction matrix given by Eq. (32) and $\langle \boldsymbol{Z}(\hat{\mathbf{q}},\,\hat{\mathbf{q}}')\rangle$ is the ensemble average of the Stokes phase matrix given by Eq. (27). The coherent Stokes column vector $\boldsymbol{I}_{\mathrm{c}}(\mathbf{r})$ satisfies the transfer equation (101).

4. Discussion

Equations (101) and (124) represent the classical form of the VRTE applicable to arbitrarily shaped and arbitrarily oriented particles and were initially introduced by Rozenberg[29] by use of simple heuristic considerations. Our detailed microphysical derivation of these equations is based on fundamental principles of statistical electromagnetics and clarifies the meaning of all participating quantities. It naturally replaces the original incident field as the source of multiple scattering in Eq. (66) by the decaying coherent field in Fig. 12(c) and leads to the introduction of the diffuse specific intensity vector $\tilde{\boldsymbol{I}}_{\mathrm{d}}(\mathbf{r},\,\hat{\mathbf{q}})$ that describes the photometric and polarimetric characteristics of the diffuse, multiply scattered light. Although our derivation assumed that the external field is a monochromatic plane wave, the linearity of Eqs. (101) and (124) implies that they are also valid for quasi-monochromatic incident light.

The physical interpretation of $\tilde{\boldsymbol{I}}_{\mathrm{d}}(\mathbf{r},\,\hat{\mathbf{q}})$ is rather transparent. Imagine a well-collimated polarization-sensitive detector centered at the observation point and aligned along the direction $\hat{\mathbf{q}}$ ($\neq \hat{\mathbf{s}}$) (Fig. 19). Let ΔS be the detector area and $\Delta\Omega$ its (small) acceptance solid angle. Each infinitesimal element of the detector surface reacts to the radiant energy coming from the directions confined to a narrow cone with the small solid-angle aperture $\Delta\Omega$ centered around $\hat{\mathbf{q}}$. On the other hand, we can use Eq. (116) to write

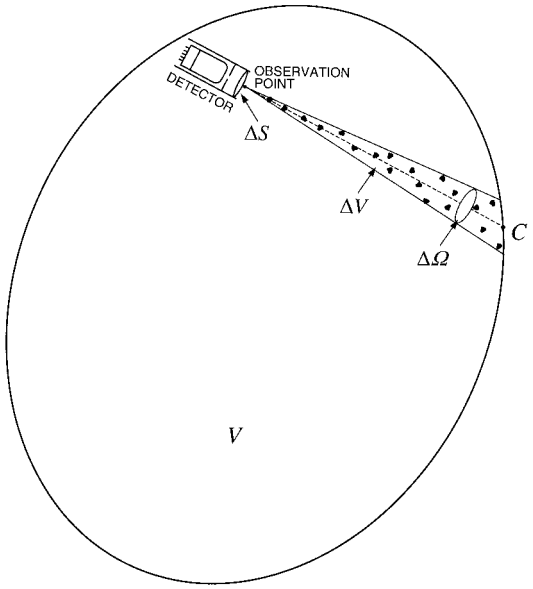

Fig. 19. Physical meaning of the diffuse specific intensity vector.

$$\Delta\Omega\tilde{\boldsymbol{I}}_{\mathrm{d}}(\mathbf{r},\,\hat{\mathbf{q}}) \approx n_0\int_{\Delta V}\mathrm{d}^3\mathbf{p}\,\frac{1}{p^2}\,\boldsymbol{H}(\hat{\mathbf{q}},\,p)\times\left[\langle \boldsymbol{Z}(\hat{\mathbf{q}},\,\hat{\mathbf{s}})\rangle\boldsymbol{I}_{\mathrm{c}}(\mathbf{r}+\mathbf{p}) + \int_{4\pi}\mathrm{d}\hat{\mathbf{q}}'\langle \boldsymbol{Z}(\hat{\mathbf{q}},\,\hat{\mathbf{q}}')\rangle\tilde{\boldsymbol{I}}_{\mathrm{d}}(\mathbf{r}+\mathbf{p},\,\hat{\mathbf{q}}')\right], \tag{125}$$

where $\mathbf{p}$ originates at observation point $\mathbf{r}$ (Fig. 18) and the integration is performed over the conical volume element ΔV having the solid-angle aperture $\Delta\Omega$ and extending from the observation point to point C as shown in Fig. 19. The right-hand side of approximation (125) is simply the integral of the scattering signal per unit surface area perpendicular to $\hat{\mathbf{q}}$ per unit time over all particles contained in the conical volume element. It is now clear which quantity describes the total polarized signal measured by the detector per unit time: it is the product $\Delta S\Delta\Omega\tilde{\boldsymbol{I}}_{\mathrm{d}}(\mathbf{r},\,\hat{\mathbf{q}})$ with the dimension of power (W). [Note that if $\hat{\mathbf{q}} = \hat{\mathbf{s}}$ then the polarized signal measured by the detector per unit time is given by $\Delta S\boldsymbol{I}_{\mathrm{c}}(\mathbf{r}) + \Delta S\Delta\Omega\tilde{\boldsymbol{I}}_{\mathrm{d}}(\mathbf{r},\,\hat{\mathbf{s}})$.] In particular, the first element of $\tilde{\boldsymbol{I}}_{\mathrm{d}}(\mathbf{r},\,\hat{\mathbf{q}})$ is the standard specific intensity $\tilde{I}_{\mathrm{d}}(\mathbf{r},\,\hat{\mathbf{q}})$ defined such that the product $\Delta t\Delta S\Delta\Omega\tilde{I}_{\mathrm{d}}(\mathbf{r},\,\hat{\mathbf{q}})$ gives the amount of radiant energy transported in a time interval Δt through an element of surface area ΔS normal to $\hat{\mathbf{q}}$ in directions confined to an element of solid angle $\Delta\Omega$ centered around $\hat{\mathbf{q}}$. The fact that one can measure the diffuse specific intensity vector with an optical device and theoretically compute it by solving the VRTE explains the usefulness of this quantity in many practical applications.

To derive the VRTE, I had to make the following approximations.

- Assume that each particle is located in the far-field zones of all other particles and that the observation point is also located in the far-field zones of all the particles that form the scattering medium.
- Neglect all scattering paths that go through a particle two and more times (the Twersky approximation).
- Assume that the position and state of each particle are statistically independent of each other and of those of all other particles and that the spatial distribution of the particles throughout the medium is random and statistically uniform.
- Assume that the scattering medium is convex, which assured that a wave exiting the medium cannot reenter it.
- Assume that the number of particles N that form the scattering medium is large and replace all factors of the type $(N - n)!/(N - n - k)!$ by N^k.
- Ignore all the diagrams with crossing connectors in the diagrammatic expansion of the dyadic correlation function (the ladder approximation).

As a consequence of these approximations, the VRTE cannot be expected to perform well for densely packed media[21] and does not describe important interference effects such as coherent backscattering. The latter is caused by constructive interference of pairs of conjugate waves that propagate along the same scattering paths but in opposite directions and is represented by diagrams with crossing connectors excluded from our derivation.[18–22]

Particles that are randomly positioned and are separated widely enough that each is located in the far-field zones of all other particles are traditionally called independent scatterers.[23] Thus our derivation explicitly demonstrates that the requirement of independent scattering is a necessary condition of validity of the radiative transfer theory.

A fundamental property of the VRTE is that it satisfies the energy conservation law. Indeed, we can rewrite Eqs. (101) and (124) as a single equation

$$\hat{\mathbf{q}} \cdot \nabla \boldsymbol{I}(\mathbf{r}, \hat{\mathbf{q}}) = \nabla \cdot [\hat{\mathbf{q}} \boldsymbol{I}(\mathbf{r}, \hat{\mathbf{q}})] = -n_0 \langle \boldsymbol{K}(\hat{\mathbf{q}}) \rangle \boldsymbol{I}(\mathbf{r}, \hat{\mathbf{q}}) + n_0 \int_{4\pi} \mathrm{d}\hat{\mathbf{q}}' \langle \boldsymbol{Z}(\hat{\mathbf{q}}, \hat{\mathbf{q}}') \rangle \boldsymbol{I}(\mathbf{r}, \hat{\mathbf{q}}'), \tag{126}$$

where $\boldsymbol{I}(\mathbf{r}, \hat{\mathbf{q}}) = \delta(\hat{\mathbf{q}} - \hat{\mathbf{s}}) \boldsymbol{I}_c(\mathbf{r}) + \tilde{\boldsymbol{I}}_d(\mathbf{r}, \hat{\mathbf{q}})$ is the full specific intensity vector. Let us now introduce the flux density vector as $\mathbf{F}(\mathbf{r}) = \int_{4\pi} \mathrm{d}\hat{\mathbf{q}} \hat{\mathbf{q}} I(\mathbf{r}, \hat{\mathbf{q}})$. Obviously, the product $\hat{\mathbf{p}} \cdot \mathbf{F}(\mathbf{r}) \mathrm{d}S$ gives the amount and the direction of the net flow of power through a surface element $\mathrm{d}S$ normal to $\hat{\mathbf{p}}$. Integrating both sides of Eq. (126) over all directions $\hat{\mathbf{q}}$ and recalling the definitions of the extinction, scattering, and absorption cross sections in Section 2.8 of Ref. 23, we obtain

$$-\nabla \cdot \mathbf{F}(\mathbf{r}) = n_0 \int_{4\pi} \mathrm{d}\hat{\mathbf{q}} C_{\mathrm{abs}}(\hat{\mathbf{q}}) I(\mathbf{r}, \mathbf{q}). \tag{127}$$

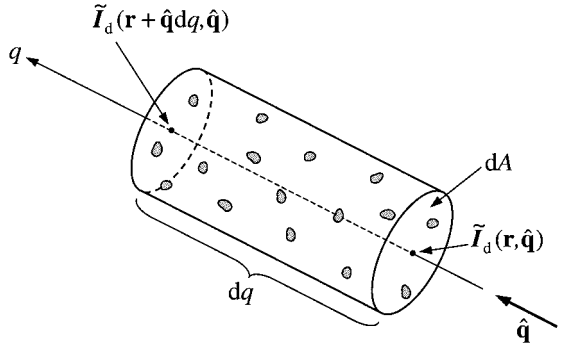

Fig. 20. Physical interpretation of the RTE.

This means that the net inflow of electromagnetic power per unit volume is equal to the total power absorbed per unit volume. If the particles that form the scattering medium are nonabsorbing so that $C_{\mathrm{abs}}(\hat{\mathbf{q}}) = 0$, then the flux density vector is divergence free: $\nabla \cdot \mathbf{F}(\mathbf{r}) = 0$. This is a manifestation of the conservation of the power flux, which means that the amount of electromagnetic energy that enters a volume element per unit time is equal to the amount of electromagnetic energy that leaves the volume element per unit time.

Equations (101) and (124) allow a simple physical interpretation (which has often been used in lieu of the formal microphysical derivation of the VRTE). Specifically, Eq. (101) shows that the change of the Stokes vector of the coherent field $\boldsymbol{I}_c(\mathbf{r})$ over the differential length $\mathrm{d}s$ is caused by extinction and dichroism, whereas Eq. (124) describes the change of the Stokes vector of the multiply scattered light $\tilde{\boldsymbol{I}}_d(\mathbf{r}, \hat{\mathbf{q}})$ as it propagates through an elementary cylindrical volume of length $\mathrm{d}q$ (Fig. 20). The first term on the right-hand side of Eq. (124) accounts for the change caused by extinction and dichroism, the second term describes the contribution of the diffuse light that illuminates the volume element from all directions $\hat{\mathbf{q}}'$ and scattered into the direction $\hat{\mathbf{q}}$ and the third term describes the contribution of the coherent light scattered into the direction $\hat{\mathbf{q}}$.

It is important to realize that the phenomenological radiative transfer theory treats the medium filled with a large number of discrete, sparsely and randomly distributed particles as continuous and locally homogeneous. It then replaces the concept of single scattering and absorption by an individual particle with the concept of single scattering and absorption by a small homogeneous volume element. Another controversial postulate of the phenomenological approach is that the scattering and absorption characteristics of the small volume element are given by the incoherent sums of the respective characteristics of the constituent particles, whereas the latter follow from the Maxwell equations. Furthermore, it assumes that the result of scattering is not the transformation of a plane incident wave into a spherical scattered wave, but rather the transformation of the specific intensity vector of the incident light into the specific intensity vector of the scattered light: $\tilde{\boldsymbol{I}}_d(\mathbf{r},$

$\hat{\mathbf{q}}) = \boldsymbol{Z}(\hat{\mathbf{q}}, \hat{\mathbf{q}}')\check{\boldsymbol{I}}_{\mathrm{d}}(\mathbf{r}, \hat{\mathbf{q}}')$, where $\boldsymbol{Z}(\hat{\mathbf{q}}, \hat{\mathbf{q}}')$ is the phase matrix of the small volume element.

An informal way to justify these assumptions is to note first that the matrices $\langle \boldsymbol{K} \rangle$ and $\langle \boldsymbol{Z} \rangle$ that enter Eqs. (101) and (124) are the same ensemble-averaged extinction and phase matrices per particle that enter the formulas of the single-scattering approximation for a small volume element (Section 3.1 of Ref. 23). Therefore, the products $n_0\langle \boldsymbol{K} \rangle \mathrm{d}q\mathrm{d}A$ and $n_0\langle \boldsymbol{Z} \rangle \mathrm{d}q\mathrm{d}A$ can indeed be interpreted as the total extinction and phase matrices of a small cylindrical volume element having a length $\mathrm{d}q$ and bases of an area $\mathrm{d}A$ (Fig. 20). Second, the product $\boldsymbol{Z}(\hat{\mathbf{n}}^{\mathrm{sca}}, \hat{\mathbf{n}}^{\mathrm{inc}})\boldsymbol{I}^{\mathrm{inc}}$ in Eq. (26) could be interpreted as the scattered polarized power per unit solid angle. Specifically, the polarized energy flow across a surface element ΔS normal to $\hat{\mathbf{n}}^{\mathrm{sca}}$ at a distance r from the particle is given by $\Delta S r^{-2}\boldsymbol{Z}(\hat{\mathbf{n}}^{\mathrm{sca}}, \hat{\mathbf{n}}^{\mathrm{inc}})\boldsymbol{I}^{\mathrm{inc}}$ and is, at the same time, equal to the polarized power scattered within the solid-angle element $\Delta\Omega = \Delta S r^{-2}$ centered at $\hat{\mathbf{n}}^{\mathrm{sca}}$. A significant residual problem with this interpretation is that two adjacent volume elements are not in the far-field zones of each other and cannot be considered independent scatterers.

It is worth emphasizing again that the detailed microphysical derivation of the VRTE described in this paper naturally leads to the definition of the Stokes column vectors $\boldsymbol{I}_{\mathrm{c}}(\mathbf{r})$ and $\check{\boldsymbol{I}}_{\mathrm{d}}(\mathbf{r}, \hat{\mathbf{q}})$, clarifies the physical meaning of all quantities that enter Eqs. (101) and (124), makes unnecessary the multiple controversial assumptions of the phenomenological approach, and allows one to reconcile the seemingly incompatible concepts of classical radiometry (light rays and ray pencils) and classical electromagnetism (electromagnetic waves, Stokes parameters, and amplitude, phase, and extinction matrices). In particular, it eliminates the need for introducing the troublesome and vague notion of an elementary volume element and provides a natural remedy for the fact that adjacent volume elements are not in the far-field zones of each other.

Methods for solving the general VRTE are discussed in Ref. 30. Equations (101) and (124) become much simpler for macroscopically isotropic and mirror-symmetric scattering media,[23] especially when one resorts to the scalar approximation,[2,6] and have been solved by use of various analytical and numerical techniques.[3–5,8,11–14]

I thank Joop Hovenier, Yuri Barabanenkov, Michael Kahnert, and Cornelis van der Mee for many fruitful discussions and an anonymous referee for useful comments. This research was funded by the NASA Radiation Sciences Program managed by Donald Anderson.

References

1. A. Schuster, "Radiation through a foggy atmosphere," Astrophys. J. **21,** 1–22 (1905).
2. V. Kourganoff, *Basic Methods in Transfer Problems* (Clarendon, Oxford, 1952).
3. S. Chandrasekhar, *Radiative Transfer* (Dover, New York, 1960).
4. V. V. Sobolev, *Light Scattering in Planetary Atmospheres* (Pergamon, London, 1974).
5. J. E. Hansen and L. D. Travis, "Light scattering in planetary atmospheres," Space. Sci. Rev. **16,** 527–610 (1974).
6. H. C. van de Hulst, *Multiple Light Scattering* (Academic, New York, 1980).
7. J. W. Hovenier and C. V. M. van der Mee, "Fundamental relationships relevant to the transfer of polarized light in a scattering atmosphere," Astron. Astrophys. **128,** 1–16 (1983).
8. J. Lenoble, ed., *Radiative Transfer in Scattering and Absorbing Atmospheres* (Deepak, Hampton, Va., 1985).
9. A. K. Fung, *Microwave Scattering and Emission Models and Their Applications* (Artech House, Norwood, Mass., 1994).
10. A. Z. Dolginov, Yu. N. Gnedin, and N. A. Silant'ev, *Propagation and Polarization of Radiation in Cosmic Media* (Gordon & Breach, Basel, Switzerland, 1995).
11. E. G. Yanovitskij, *Light Scattering in Inhomogeneous Atmospheres* (Springer-Verlag, Berlin, 1997).
12. G. E. Thomas and K. Stamnes, *Radiative Transfer in the Atmosphere and Ocean* (Cambridge University, New York, 1999).
13. K. N. Liou, *An Introduction to Atmospheric Radiation* (Academic, San Diego, Calif., 2002).
14. J. W. Hovenier, C. V. M. van der Mee, and H. Domke, *Transfer of Polarized Light in Planetary Atmospheres* (Kluwer Academic, Dordrecht, The Netherlands, to be published).
15. A. G. Borovoy, "Method of iterations in multiple scattering: the transfer equation," Izv. Vyssh. Uchebn. Zaved. Fiz., No. 6, 50–54 (1966).
16. Yu. N. Barabanenkov and V. M. Finkel'berg, "Radiation transport equation for correlated scatterers," Sov. Phys. JETP **26,** 587–591 (1968).
17. A. Z. Dolginov, Yu. N. Gnedin, and N. A. Silant'ev, "Photon polarization and frequency change in multiple scattering," J. Quant. Spectrosc. Radiat. Transfer **10,** 707–754 (1970).
18. L. A. Apresyan and Yu. A. Kravtsov, *Radiation Transfer* (Gordon & Breach, Basel, Switzerland, 1996).
19. A. Lagendijk and B. A. van Tiggelen, "Resonant multiple scattering of light," Phys. Rep. **270,** 143–215 (1996).
20. A. Ishimaru, *Wave Propagation and Scattering in Random Media* (Institute of Electrical and Electronics Engineers, New York, 1997).
21. L. Tsang and J. A. Kong, *Scattering of Electromagnetic Waves: Advanced Topics* (Wiley, New York, 2001).
22. V. P. Tishkovets, "Multiple scattering of light by a layer of discrete random medium: backscattering," J. Quant. Spectrosc. Radiat. Transfer **72,** 123–137 (2002).
23. M. I. Mishchenko, L. D. Travis, and A. A. Lacis, *Scattering, Absorption, and Emission of Light by Small Particles* (Cambridge University, New York, 2002).
24. A. P. Prishivalko, V. A. Babenko, and V. N. Kuzmin, *Scattering and Absorption of Light by Inhomogeneous and Anisotropic Spherical Particles* (Nauka i Tekhnika, Minsk, USSR, 1984), in Russian.
25. L. L. Foldy, "The multiple scattering of waves," Phys. Rev. **67,** 107–119 (1945).
26. M. Lax, "Multiple scattering of waves," Rev. Mod. Phys. **23,** 287–310 (1951).
27. V. Twersky, "On propagation in random media of discrete scatterers," Proc. Symp. Appl. Math. **16,** 84–116 (1964).
28. D. S. Saxon, "Lectures on the scattering of light," Science Report No. 9 (Department of Meteorology, University of California, Los Angeles, Los Angeles, Calif., 1955).
29. G. V. Rozenberg, "Stokes vector-parameter," Usp. Fiz. Nauk. **56**(1), 77–110 (1955).
30. M. I. Mishchenko, "Multiple scattering of light in anisotropic plane-parallel media," Transp. Theory Stat. Phys. **19,** 293–316 (1990).